Numerical Design on Annular Dump Combustor of a Ship

A thesis submitted in partial fulfillment of the requirements for the award of degree of

MASTER OF TECHNOLOGY

in Marine Engineering & Management

by

VAIBHAV SONI

(Reg.No.2001215007)

Under the guidance of

Dr. SUJOY SAHA

Faculty of Mechanical Engineering

Indian Maritime University, Kolkata (A Central University, Govt. of India)

(Ex. Associate Professor, Academy of Technology, Hooghly)

Department of Marine Engineering, Indian Maritime University Kolkata Campus

Kolkata-700088.

August 2022

INDIAN MARITIME UNIVERSITY KOLKATA CAMPUS

Department of Marine Engineering

CERTIFICATE

This is to certify that the thesis entitled "NUMERICAL DESIGN ON ANNULAR DUMP COMBUSTOR OF A SHIP" submitted by VAIBHAV SONI to the Indian Maritime University Kolkata Campus for the award of the degree in Master of Technology and Management in Marine Engineering is a bonafide record of the project work carried out by him under our supervision. The contents of this thesis, in full or in parts have not been submitted to any other institute or University for the award of any degree or diploma.

The Project has been carried out at Indian Maritime University Kolkata Campus.

Dr. Sujoy Saha	Dr. Deepak Mishra	External Examiner
Project Guide	Course coordinator	
Faculty of Mechanical Engineering, IMU-KC	Indian Maritime University.	
(Ex. Associate Professor, Academy of Technology, Hooghly)	Kolkata Campus.	

EVALUATION SHEET

Name of the candidate	VAIBHAV SONI
Title of the project	NUMERICAL DESIGN ON DUMP COMBUSTOR OF A SHIP
Specialization	MARINE ENGINEERING & MANAGEMENT
Date of Examination	22 AUGUST, 2022

This thesis is approved by the Board of Examiners

External Examiner :

Internal Examiner :

Contents

ACKNOWLEDGEMENTS i
TABLE OF FIGURES ii
ABSTRACT iii
INTRODUCTION 1
MATHEMATICAL FORMULATIONS 21
2.1 Computational domain: 21
2.2 Governing Equations for Turbulent Flow: 22
2.3 Boundary Conditions: 23
2.4 Numerical Methodology: 23
2.5 Validation: 24
RESULTS AND DISCUSSION: 25
3.1 Study of Streamline Contours: 25
3.1.1 Stream line contours for simple dump combustor: 25
3.1.2 Stream line contours for dump combustor with rectangular restriction: 27
3.2 Variation of axial velocity profiles for different value of Reynolds number: 31
3.2.1 Simple dump combustor. 31
3.2.2 Dump combustor with rectangular restriction. 32
3.2.3 Dump combustor with rectangular curved restriction. 33
3.2.4 Dump combustor with spherical restriction. 35
3.2.5 Dump combustor with diagonal restriction. 37
3.3 Variation of axial velocities at centerline due to different restrictions: 38
3.4 Variation of axial velocity profiles for different combustors at Re = 10^5: 40
CONCLUSION 42
NOMENCLATURE 43
PUBLICATIONS FROM THIS THESIS 43
REFERENCES 44

ACKNOWLEDGEMENTS

It is my proud privilege to acknowledge the help and guidance received in preparation and presentation of this report. It would not have been possible to prepare this report in this form without valuable help, cooperation and constant guidance. First and foremost, I wish to record my sincere gratitude to Department of Marine Engineering, IMU Kolkata and to respected Director Shri Arun K Eswara, Indian Maritime University for the support and encouragement in preparation of this report and making available library and laboratory facilities to prepare this report.

My sincere thanks to Professor and guide Dr. Sujoy Saha, Department of Mechanical Engineering, IMU Kolkata, for his detailed suggestions, reviews and sharing his valuable time by guiding me on investigations and presentation for this research work throughout the period of this report.

I express my sincere gratitude to Course coordinator, Dr. Deepak Mishra and Mr. R. Prasanna Kumar, HOD Department of Marine Engineering, IMU Kolkata, for their motivation and support in completion of the project report.

TABLE OF FIGURES

Figure 1. Computational domain of simple dump combustor without any restriction. 21

Figure 2. Computational domain of modified dump combustor with rectangular cavity. 21

Figure 3. Computational domain of modified dump combustor with rectangular curved cavity. 22

Figure 4. Computational domain of modified dump combustor with semi- hemispherical cavity. 22

Figure 5. Computational domain of modified dump combustor with diagonal cavity. 22

Figure 6. Axial velocity profile of the present work and the work 24

Figure 7. Streamline contour comparison of simple dump combustor for different Reynolds number. 26

Figure 8. Streamline contour comparison of dump combustor with rectangular restriction for different Reynolds number. 27

Figure 9. Streamline contour comparison of dump combustor with rectangular curved restriction for different Reynolds numbers. 28

Figure 10. Streamline contour comparison of dump combustor with semi hemispherical restriction for different Reynolds number. 29

Figure 11. Streamline contour comparison of dump combustor with diagonal restriction for different Reynolds number. 30

Figure 12. Variation of axial velocity profiles at different axial positions on x- axis for a simple dump combustor. 31

Figure 13. Variation of axial velocity profiles at different axial positions on x- axis for dump combustor with rectangular cavity. 32

Figure 14. Variation of axial velocity profiles at different axial positions on x- axis for dump combustor with rectangular curved restriction. 34

Figure 15. Variation of axial velocity profiles at different axial positions on x- axis for dump combustor with semi hemispherical restriction. 36

Figure 16. Variation of axial velocity profiles at different axial positions on x-axis for dump combustor with diagonal restriction. 37

Figure 17. Variation of Centerline velocity for dump combustor without and with restriction. 39

Figure 18. Variation of Axial velocity profile along the radial direction at x = 0.10 m. .. 41

ABSTRACT

In this work, a numerical investigation has been performed on the flow characteristics of a fluid flowing through a simple annular dump combustor and modified dump combustor with certain central restrictions like rectangular, curved, semi hemispherical and diagonal shape. The restrictions are located at a fixed distance of 0.14m from the inlet. Flow characteristics and patterns are presented sequentially in the form of streamline contours, axial velocity profile and the centerline velocity profiles. The above mentioned flow characteristics are studied at several locations in the flow field with considering Reynolds number ranging from 10^3 to 10^6 for different models. The governing two dimensional partial differential equations for conservation of mass and momentum are discretized with the help of control volume based finite volume method. The discretized equations are solved iteratively by SIMPLE algorithm with the help of upwind scheme for a fixed aspect ratio of 3 and central restriction of 120%. The analysis corroborates and concludes that, more numbers of bubbles are formed in a geometrically modified dump combustor than in a plain dump combustor. It has been also noted that the number of recirculating bubble increases with increasing Reynolds number. Consequently, central recirculating zone is enhanced, which ensure desirable mixing of fluids in ship combustor and helps significantly in reduction of NOX emission and combustion residuals. In order to authenticate the present work, validation is also carried out and presented in the sub section.

CHAPTER 1

INTRODUCTION

The development of combustion systems of marine propulsion is able to meet the future drastic standardization requirements on the reduction of the level of harmful emissions which heavily relies on the new concepts of combustion chamber modification and technologies. High efficiency and low emission combustion technology have been a requirement for realistic industrial combustors. Flame stability and fuel mixing is a fundamental parameter in combustion. A combustor must contain and maintain stable combustion despite very high air flow rates. To do so, combustors are carefully designed to mix with the air and fuel properly for the combustion process with the least residuals. Flow with recirculation increases the mixing intensity and stabilizes the flame. Also, the advantage of enhanced mixing is the reduced peak temperature and consequently, the possibility of an additional reduction of thermal NO_x emission. For better mixing of fuel and air in the combustion chamber, proper optimization in performance, the flow characteristics of fluid passing through different types of annular dump combustor models are studied extensively in the present work. The outcome of the literature review is placed considering plain dump combustor configuration and plain dump combustor configuration with some modifications separately. In order to understand the effect of fluid flow through plain dump combustor configuration, different researchers have performed theoretical and experimental investigations. Among them, Tsui and Shu (1998) have numerically investigated the buoyancy effects on the flow through a symmetric sudden expansion duct. They have considered the Reynolds number 56 and 114, and Grashof number from 0 to 50,000 for fixed expansion ratio of 3. They have presented their results into two parts. Firstly, the duct system is placed vertically such that the flow is assisted by buoyancy force. Then, the duct is rotated to examine the effects of orientation. They have assumed that the flow is steady, 2-D and laminar. They have considered a fully developed velocity profile with a uniform temperature at inlet. In their numerical analysis, they have obtained difference analogues of the governing equations by using the finite volume method. They have constructed a code based on non-orthogonal, non-staggered griding arrangements. In the discretization, the flow convection is approximated by the linear upwind difference method. The pressure gradients are approximated by central differencing scheme using the

nearby nodal pressures. When the duct is placed vertically, they have observed that the flow field remains symmetric throughout the Grashof number range (Gr =100 to 10000) for Re = 56. A pair of recirculating flow appears near the centerline as Grashof number becomes sufficient large. At Re = 114, the asymmetric flow is transformed to become symmetric at low Grashof numbers. They have seen that, when the duct is inclined to the vertical position, a symmetric flow pattern is obtained at $\gamma = 60^{o}$ (inclination angle from the vertical axis). They have also observed that, in the horizontal position ($\gamma = 90^{o}$), different sizes of recirculating bubbles appear behind each side of the expansion.

Hammad et al. (1999) have carried out a combined experimental and computational study to investigate the flow characteristics of a nonlinear visco-plastic fluid through an axisymmetric sudden expansion. They have considered axisymmetric 2:1 (based on radii) expansion during their measurements and computations. They have used a fixed Hedstrom number of 1.65 and the Reynolds number ranging from 1.8 to 58.7. During experiment, they have used particle image velocimetry (PIV) technique and flow visualizations to measure two dimensional distribution of axial and radial velocity. From these measurements, they have calculated stream function at the separated, reattached and redeveloping flow regions. In their numerical study, they have solved the fully elliptic governing equations by using finite-difference approximations. For the calculations, they have assumed fully developed flow at inlet and exit plane. From the experimentally obtained velocity vector, they have compared the corner recirculation flow of the non-Newtonian and Newtonian fluid. After comparison, they have seen that the strength of the recirculating flow for the non-Newtonian fluid is weaker than that of the Newtonian fluid. They have seen that there is no flow recirculation in the expansion corner for small Reynolds numbers (approximately Re < 17) of the non-Newtonian flow for both the experiments and the computations. But, for the case of Re = 17.4 and higher, a recirculating flow region exists.

Khezzar et al. (1999) have experimentally performed to quantify the isothermal and combusting flows downstream of a plane sudden expansion. They have used an area ratio of 2.86 and a Reynolds number of 20000. They have used optical access for flow visualization and laser Doppler velocimetry for velocity measurement. They have considered the combusting flows comprising of premixed methane and air, over a range of equivalence ratios 0.72 and 0.92. They have seen that the extent of asymmetry of the isothermal flows can be reduced by coupling the pressures between the two recirculation

regions. They have studied the periodic variations of flame shape, velocities, acceleration, and temperature with the dominant pressure oscillation of rough combustion. During their study, variation of recirculation length is observed from less than 0.5 to 3 step heights. They have seen that the concentration of NOx decreases at the duct exit with increase in the amplitude of flow oscillation, natural or imposed.

Yokoyama et al. (1999) have experimentally and numerically studied the forced and mixed convective heat transfer in a liquid saturated horizontal porous duct with a sudden expansion configuration. They have considered a heated region on the lower surface downstream and adjacent to the expansion. The flow is assumed by them as steady, laminar, incompressible and two-dimensional. The Rayleigh number (Ra) ranging from 50 to 500 and Peclet numbers (Pe) in the range of 0.1 to 100 are used by them. They have used finite difference method to solve the governing equations following the upwind differencing procedure described by Gosman et al. (1969) and Patankar (1980). They have considered both Darcy's and non-Darcy's formula. The Gauss-Seidel point iterative method is used by them to solve the resulting system of algebraic equations for Darcy's case, and line-by-line method for non-Darcy's case. The convergence criterion is considered by them as 10^{-4} for Ra > 100 and 10^{-5} for Ra < 100. At the inlet, they have assumed that the flow is fully developed. At the exit, the horizontal gradients of stream function, vorticity, and temperature are assumed by them as zero. During their experimental investigation, they have used thin foil heater to supply heat and thermocouple with data acquisition system to measure the temperature. They have observed that the non-Darcy effects reduce the heat transfer coefficient, but the difference from the Darcy's case is approximately four percent. They have concluded that the non-Darcy's case has no effect on the flow and temperature field with their considered porous structure and fluid.

Tavoularis and Singh (1999) have numerically studied the flow characteristics of laminar pulsatile flow through axisymmetric sudden expansions. They have considered diameter ratios of 1:2.25 and 1:2.00, time averaged bulk Reynolds number over the range of and Womersley number. They have used the commercial CFD code FIDAP to solve the time dependent Navier-Stokes equations for an incompressible Newtonian isothermal fluid without body force. In their numerical approach, they have assumed boundary conditions as zero radial and azimuthal velocities at the inlet, no-slip conditions at the wall, the zero radial velocity along the axis of symmetry, and a uniform velocity at the inlet. For steady flow, they have seen that the recirculation zone length increases linearly with increase in

Reynolds number. For pulsatile flow, particularly at higher values of W, they have observed that the recirculation zone length strongly depends on the acceleration of the flow and not with the instantaneous Reynolds number. This recirculation zone length increases during the deceleration phase and decreases during the acceleration phase. They have seen that, at low Re (Re < 25), the vortex remains always attached, irrespective of pulsation frequency. They have also seen that, at very low W, the vortex also remains attached, irrespective of the value of Re (Re < 400). They have suggested that, even in this low W-range, vortex detachment may occur if the pulsatile waveform causes higher acceleration than they have considered.

Schreck and Schafer (2000) have numerically studied bifurcation phenomena in three dimensional sudden channel expansions. In their numerical approach, they have used steady incompressible Navier-Stokes equation and SIMPLE algorithm. At the inlet, a fully developed channel flow is used. At the outlet, they have assumed normal derivatives of all three velocity components to be zero. They have considered Reynolds number ranging from 70 to 105 for an expansion ratio of 1:3. They have studied bifurcation from the steady symmetric solution to steady asymmetric solutions. They have seen that at low Reynolds numbers the recirculation zones are fully symmetric and increase in size with increase in Reynolds number. After crossing the bifurcation point, there exist a small and a large recirculation zone. With further increasing Reynolds number, the small zone first becomes smaller and finally remains constant in size, while the large zone continuously becomes larger. They have considered three different channel geometries. These are (w and H are channel width and height at exit, respectively). They have seen that, at narrower channel width, bifurcation point moves to higher Reynolds number. The narrower the channel (for fixed Reynolds number) the reattachment length becomes smaller.

Guo et al. (2001) have performed numerical simulation of unsteady turbulent flows behind axisymmetric sudden expansion configuration. They have considered expansion ratio (E) in the range from 1.96 to 6.0 and Reynolds number (Re) from 50,000 to 200,000. They have used VLES approach and the standard k-ε model. They have solved three-dimensional, unsteady, Reynolds-averaged Navier-Stokes equations by a finite volume formulation. They have used three-dimensional structured grid with small orthogonality deviations. At the inlet and exit, they have assumed a fully developed velocity profile. For all walls, they have used a universal log-law wall function. They have observed two modes of oscillations for the range of expansion ratios from 3.0 to 6.0. These oscillations are a combination of a

regular precession and a flapping motion in a rotating frame. They have seen that the precession mode exhibits a stronger oscillation intensity of flow variables than the flapping mode in the whole field. They have also observed that a bifurcation point appears when the expansion ratio is around 3.95. For the case of E =6.0, they have seen that a complex oscillation occurs in the flow when Re is 8.34 $\times 10^4$ or less. They have concluded that a critical Reynolds number occurs which is correlated with the expansion ratio. Above this Reynolds number a regular pattern of oscillation remains permanently. Ko and Sung (2001) have numerically studied turbulent flow behavior inside a cylindrical combustion chamber with modified sudden expansion configuration. They have considered a flame holder downstream of the sudden expansion to promote turbulent mixing and to accommodate flame stability. They have chosen three different type of flame holder. These are disc type, cutting plane type and cutting plane with shaft type. The Reynolds numbers of 5000 to 50000, based on the bulk velocity and the diameter of the inlet pipe, are considered by them. During numerical analysis, they have used large eddy simulation (LES) code. They have solved governing equations in a general co-ordinate system based on the physical contravariant velocity components. In their simulation, they have used Smagorinsky model proposed by Smagorinsky (1963) and the Lagrangian dynamic subgrid-scale (SGS) model proposed by Meneveau et al. (1994). Van Driest (1956) damping friction is also used to reduce the length scale in the near wall region. They have used second-order Adams-Bashforth scheme for time discretization. The second-order central difference scheme is used by them for the diffusive and convective term. For pressure field deduction, they have used HSMAC (highly simplified marker-and-cell) method (Hirt and Cook, 1972). They have used a wall boundary condition by a generalized wall function which is proposed by Morinishi and Kobayashi (1991). At the outlet, they have imposed convective boundary condition which is proposed by Dai et al. (1994). They have also performed an experimental investigation for comparison with the theoretical results. During their experiment, laser Doppler velocimetry measurement is carried out in a circular water channel to measure axial and radial velocity components. They have observed that the position of the peak velocity is significantly shifted toward the centerline of the cylinder combustor to an extent depending on the type of flame holder. This position closely associated with the size of the recirculation region, behind the flame holder, is also observed by them. In the case of the CPWS, they have seen that a small recirculation zone is formed in the front corner of the flame holder. This yields the smallest size of recirculation zone behind the flame holder and

the ring-type vertical structure is maintained for a long time. They have noted that two axisymmetric vortex rings with opposite rotations are formed behind the flame holder. The inside vortex ring is with greater intensity than the outside one. These two-ring-type vortices are deformed at the downstream and the stream-wise vortices are generated at the shear layer of the inner vortex region, which is observed by them.

Chakrabarti et al. (2002) have numerically carried out the performance simulation of a vortex controlled diffuser in low Reynolds number regime. They have considered a sudden expansion configuration with suction slot on different position of vertical and horizontal walls. They have used Reynolds number ranging from 20 to 100, aspect ratio for 2 and 4, and bleed fraction for 2 per cent, 5 per cent and 10 per cent. During numerical simulation, two dimensional steady differential equations for conservation of mass and momentum are solved by finite difference method. Power law scheme is used to discretize the convective terms. They have used SIMPLE algorithm with line by line ADI method. At the inlet and exit, fully developed boundary condition and at the wall no slip condition is used by them. They have observed that static pressure rise increases with increase in bleed. For a given Reynolds number and aspect ratio, the diffuser efficiency increases with increase in bleed fraction is noted by them. They have established that the position of the bleed slot should be located preferably at the vertical wall top corner of the vortex controlled diffuser for the best performance.

Paschereit and Gutmark (2002) have experimentally studied the performance of a gas turbine combustor having sudden expansion configuration with inlet modification. At the upstream of the sudden expansion they have used miniature vortex generators which are small triangular ramps. The height of the miniature vortex generator is approximately equivalent to twice the boundary layer thickness. The miniature vortex generators are installed at the circumference to interfere with the roll up of the vortices at sudden expansion region through the induction of stream-wise vorticity. They have seen that the stream-wise vorticity interacts with the circumferential vorticity, causing azimuthal deformation and excitation of high-order azimuthal modes that disrupts the formation of coherent circumferential vortices. They have used two filtered fiber optic probes to detect OH chemiluminescence for time varying heat release. To study the flame structure, flow visualization system is used. Several modes of instabilities are identified by them. These are axisymmetric low frequency instabilities at external recirculation zone downstream of the dump plane, helical low frequency instabilities at central recirculation zone which is

formed by vortex breakdown and high-frequency helical instabilities occurs when the power level is increased or when the air inlet temperature is reduced. They have observed that, by the use of miniature vortex generator, low frequency instabilities are reduced by 50% and high-frequency oscillations are suppressed by up to 28 dB. Emissions of NOx are also reduced by a factor of 2.

Galvin and Fitzpatrick (2002) have experimentally observed strong acoustic interactions in a premixed dump combustor having configuration of plane sudden expansion. They have considered Reynolds number in the range of 1.5×10^4 to 2×10^4 and two different expansion ratios of 18:1 and 12:1. They have used optical access for flow visualization and Kistler piezo-electric pressure transducer with a range of 0-10 bar for instantaneous pressure measurement. They have observed both thermo-acoustic and flow/acoustic interactions. They have seen that oscillations occur at a number of frequencies which are related to the acoustic properties of the exhaust duct, the upstream mixing can and the overall geometry. They have performed their experiments in two different modes. These are lower power levels and higher power levels. For lower power levels, they have seen resonance occur at both the upstream mixing can and downstream exhaust. For higher power levels, the combustion is very unstable and oscillation of the flame front is clearly visible.

Pinho et al. (2003) have numerically studied pressure losses in the laminar non-Newtonian flow of shear-thinning power-law fluids through an axisymmetric sudden expansion. They have used a diameter ratio of 1 to 2.6 and Reynolds number ranging from 0.1 up to order 200. They have used a uniform velocity profile at inlet. At outlet, they have assumed zero axial gradients to all variables (except pressure) and at walls, no slip conditions. To solve the governing equations, they have developed a CFD code which is based on the finite volume method applied to non-staggered meshes. They have considered central difference scheme for diffusion terms and second order upwind for the convection terms. They have considered the pressure velocity coupling with a time marching form of the SIMPLEC algorithm. They have fixed convergence criteria for all calculations when normalized residual is less than. They have assessed the effects of shear thinning and Reynolds number on pressure loss. They have studied the variation of the recirculation length and the eddy strength. They have observed that the normalized recirculation length decreases with shear thinning. They have also observed that the eddy strength reduces with shear thinning and also exhibits an asymptotic value at low Reynolds number. They have seen that at low Reynolds number, the flow is dominated by viscous forces and the local loss coefficient

varies inversely with the Reynolds number.

Smith (2004) has experimentally studied the pressure recovery for a steady flow through a rectangular channel with rounded sudden area expansion. He has used Reynolds number in the range of 300<Re<25,000 and aspect ratio in the range of 7.5<AR<40. During experiment, flow visualization is performed using a double pass system for image. Velocity is measured by using a single, straight, hot wire probe. He has measured pressure using a capacitance manometer. He has seen that the channel flow expands and decelerates upstream of the exit plane resulting in large pressure recovery, especially for turbulent channel flow. The rounded exit radius in turbulence levels as much as 25% higher than sharp edged exits is noted by him.

Behrens et al. (2005) have experimentally studied the combustion characteristics in a modified backward-facing step combustor using countercurrent shear to enhance the turbulent burning velocities. In modified configuration, they have considered a suction slot of 0.25 times of channel inlet height located immediately below the trailing edge. A secondary flow is pulled from the combustor via a suction pump. They have considered two combustors geometry; one is modified step geometry and another is baseline geometry. For modified step geometry, a step extension of length L and corner chamfering at an angle α at the inner edge of sudden expansion with suction immediately below the trailing edge are considered. For baseline geometry (L=α=0), sudden expansion with suction immediately below the trailing edge is considered by them. The Reynolds number (based on step height) of 1.2×10^4, corresponds to mean velocity of 12.5 m/s, is considered by them during experiments. They have considered a rectangular channel with expansion ratio of 2:1. They have used Particle image velocimetry (PIV) to measure heat release rate under isothermal flow conditions. Using chemiluminescence measurements, they have seen that for base geometry the relative heat release rates increase by 90% with a counter flow level of 6% of the primary flow by mass. For modified step geometry, 150% increase of heat release rates with a counter flow level of 2.4% is observed by them. They have also observed that relative heat release rates drops off sharply as secondary mass flow levels exceeds 2.5% of the primary mass flow.

Forliti and Strykowski (2005) have experimentally studied the control of isothermal turbulent flow within a reward facing step combustor using countercurrent shear. They have used a suction base approach to achieve countercurrent shear control. Suction slot is placed at the vertical wall and near the inner edge of the sudden expansion plane. They have

considered suction flow up to approximately 10% of the primary flow. For all experiments, a constant Reynolds number of 13600, corresponding velocity of approximately 12.5 m/s is considered by them. They have observed that peak turbulence levels increase with increase in suction. They have seen that counter flow has an effect of augmenting the natural reverse flow, caused by the sudden expansion of the step. Augmentation in the recirculation is explained by them as both an increase in strength of the reverse flow, as well as a movement of the strong recirculation zone upstream, where the mean velocity gradients are higher and turbulent production is enhanced.

Palm et al. (2006) have experimentally and numerically studied the turbulent swirling flow characteristics in a modified sudden expansion combustor. At the inlet of the sudden expansion, they have considered concentric annular pipe configuration with swirl generator. They have considered Reynolds number ranging from 50,500 to 125,500, for annular flow and from 23,500 to 102,000 for main flow. Swirl number (S) in the range of 0 to 1.2 for expansion ratio of 1.5 and 2.0 are used by them. A two-velocity component laser Doppler instrument is used to measure velocity profile across the annular channel entrance. Complementary to the experimental investigations, they have also conducted a computational study. During their numerical study, they have applied both Reynolds-Averaged Navier-Stokes (RANS) approach and Large-Eddy Simulation method. Separate 3D and 2D, axisymmetric RANS computations of the swirl flow is considered by them. When they have considered 2D axisymmetric problem, they have used SIMPLE algorithm to couple the velocity and pressure fields. They have considered orthogonal grids and collocated variable arrangement. A central differencing scheme is used for the approximation of diffusive fluxes and a blended upwind-central differencing scheme is considered by them for the discretization of convective fluxes. For 3D axisymmetric problem, the code FASTEST, based on a finite volume numerical method for solving the three dimensional filtered Navier–Stokes equations on block-structured and body-fitted meshes, is used by them. SIMPLE algorithm is applied for coupling the velocity and pressure fields. They have used second-order central differencing scheme for the spatial discretization and the second-order Crank–Nicolson method for the time discretization. No-slip boundary conditions are applied at both walls. They have observed that the axial velocity profile becomes increasingly asymmetric with increase in swirl intensity. The axial velocity increases from the inside to outside wall of the annular flow as a consequence of the increase in swirl intensity. They have seen that the maximum tangential velocity is

formed approximately in the middle of the annular channel.

Abu-Nada et al. (2007) have carried out numerical investigation of heat transfer and fluid flow over a backward facing step configuration under the effect of suction and blowing. In their configuration, part of the channel's bottom wall, adjacent to the step, is considered permeable and constant uniform velocity is allowed to bleed through it. They have used Reynolds number in the range of 200 to 800 and bleed coefficient ranging from -0.005 to 0.005 for an expansion ratio of 2. The flow is assumed by them as two-dimensional, steady, incompressible and having constant fluid properties. They have used finite volume method to solve the non-dimensional continuity, momentum and energy equations. During computation, SIMPLE algorithm is used by them. The diffusion term in the momentum and energy equations is approximated by second-order central difference scheme. They have adopted a second-order upwind difference scheme for the convective terms. At the inlet and outlet fully developed velocity profile is used by them. A no-slip condition is applied at the top wall of the channel, vertical wall of the step and the bottom wall except where the normal bleed velocity is imposed. They have observed that the reattachment length of the primary recirculating bubble increases by increase in blowing bleed coefficient and decreases by increase in suction bleed rate. They have also observed that suction increase the size of the secondary bubble and blowing reduces it.

Duwig and Fureby (2007) have numerically studied strong flame instability in a sudden expansion combustor with inlet modification. The inlet section is divided into two approach channels by a splitter plate that ends in a tip having an opening angle of 14o. The tip of the splitter plate is located at a certain distance upstream of the dump plane. They have used propane (C3H8) as fuel. Reynolds number based on dump plane height is considered by them as 25,000. They have used reactive Navier-Stokes equations (rNSE) to describe the turbulent combustion. To solve governing equations, they have considered finite volume and finite difference methods separately. When finite volume method is considered by them, high-order reconstruction of convective fluxes and central differencing of inner derivatives with second-order accuracy is used. Crank–Nicholson time-integration with second-order accuracy is used for time derivatives. For pressure–velocity coupling, they have used PISO method proposed by Issa (1986). During finite difference method, they have used a fourth-order centered scheme for spatial discretization, except for the convective terms. A fifth-order weighted non-oscillatory scheme proposed by Jiang and Shu (1996) is used for the convective terms ensuring stability and high-order accuracy. A

second-order finite difference scheme is used for time discretization. At the walls, no-slip conditions are used. They have noted that the reaction zone is formed by two flame-brushes anchoring in the shear layers that develop at the step corners. In these shear layers, large-scale (i.e., macroscopic) mixing takes place between cold reactants and hot products.

Kodama et al. (2007) have performed numerical simulation on unsteady turbulent flow for a two-dimensional backward facing step configuration with periodic perturbation (i.e., injection and suction). They have placed an injection/suction slot at the inner edge of sudden expansion plane, which has a width of 1 mm. The flow direction through this injection/suction slot is 45 degrees to the main stream. They have considered expansion ratio of 1.5 and Reynolds number of 3.7 103, based on mean velocity at the center of the channel inlet and the channel inlet height. Reynolds-averaged continuity and Navier Stokes equations are used by them as governing equations during computations. They have adopted low Reynolds number type k-ε turbulence model proposed by Shimada and Nagano (1996). All the convective terms in the governing equation are discretized by the third-order upwind scheme proposed by Kawamura and Kuahara (1984). They have used second-order central difference scheme for all other spatial derivatives. At the inlet and outlet, fully developed velocity profiles are considered by them. On the wall, no slip condition is used. They have observed that the vortex generated by the periodic perturbation is governed by the inviscid convection effect. They have suggested that, if the ratio of turbulent diffusion to convection with in the free shear layer downstream of the step is less than approximately 0.1, the unsteady nature in the flow field can reasonably be predicted.

Strakey and Yip (2007) have experimentally and numerically investigated the vortex flow characteristics of a swirl stabilized dump (sudden expansion) combustor under cold flow conditions. At the inlet region of the dump combustor, they have considered a center-bodyswirler which forms a concentric annular geometry in this region. The blockage ratio of the swirler (area in the annulus/ the total open area of the slots) is 3.0. During experimental investigation, they have used two-dimensional particle image velocimetry (PIV) to measure axial, radial and tangential velocity components. A numerical study is performed, to understand the complex hydrodynamics which is observed in their experiments. They have used both Large-Eddy Simulation method and Reynolds-Averaged Navier-Stokes (RANS) techniques. A finite volume based commercial CFD code FLUENT 6.2 is used during numerical study. The nominal velocity of 54 m/s and a flow rate of 0.137 kg/s are considered by them. They have observed that the expansion of the jet and the

ensuing breakdown of the vortex results in a central recirculation zone as well as corner recirculation zone.

Uruba et al. (2007) have experimentally investigated on control of narrow channel flow behind a modified backward facing step. They have incorporated suction/blowing at the outer corner edge of the vertical wall. They have considered two orifice shape slots that are rectangle and serrated. They have used suction/blowing flow coefficient (CQ, negative for suction and positive for blowing) from -0.035 to 0.035. The Reynolds number based on the hydraulic diameter of the inlet channel is considered by them as 5×10^4 while that based on step height, is approximately 3.5×10^4. The main flow parameters are measured by them with the help of a Pitot-static tube. Static pressure distribution on the bottom wall downstream from the step is measured with 0.4 mm diameter orifices. They have observed that both suction and blowing are effective in shortening the recirculation zone. They have seen that suction effectiveness is relatively insensitive to the slot profile, while that of blowing strongly depends on the slot geometrical parameters. Reduction of the recirculation zone length is more effective for smaller slot cross-section keeping the same CQ value, which is observed by them. They have noted that shape of the slot orifice is not very important, serrated shape gives slightly shorter recirculation zone than rectangular one for the same blowing rate and orifice cross-section. They have seen that both blowing and suction are able to reduce the length of the separation zone down to one third of its value without control.

Vanierschot and Bluck (2007) have experimentally investigated the influence of swirl on the mean cold flow field of a modified sudden expansion configuration. At the inlet region of the sudden expansion, they have considered a central restriction which creates an annular channel up to the sudden expansion plane. The outlet of the annular channel is formed by a stepwise expansion followed by a divergent portion with opening angle α=200. This divergent portion is again followed by a sudden expansion with a ratio of infinity (free jet). The Reynolds number based on the mean axial velocity and the difference in diameter of the annular channel is considered as 11000. They have measured axial and azimuthal velocity simultaneously using a dual beam Laser Doppler Anemometry (LDA) system in forward scattering mode. They have studied the mean axial velocity profile and maximum magnitude of velocity at different axial location for varying swirl number. During their experiment, swirl number (S) is varied from 0 to 0.9. They have observed that the central rod of the annular duct acts as a bluff body to the flow which creates a central recirculation

zone. The stagnation point of this central recirculation zone lies below an axial position x/D_0=0.61. At a distance x/D_0=2.16, the maximum velocity is again situated along the axis. At critical swirl number, they have observed that the axial pressure gradient is large enough to create backflow along the central axis and vortex breakdown occurs. At high Reynolds numbers, they have seen two different types of breakdown. These are axisymmetric (bubble) breakdown and spiral breakdown.

Chakrabarti et al. (2008) have carried out numerical simulation on the performance of a modified sudden expansion configuration, viewed as a diffuser. In modification, they have considered a fence downstream of the throat of sudden expansion with a fixed fence subtended angle of 10^0. They have considered Reynolds number ranging from 20 to 100, and distance of fence from throat from 0.2 to 2 for the aspect ratio of 2. During numerical simulation, two dimensional steady differential equations for conservation of mass and momentum are solved by finite difference method. Power law scheme is considered by them to discretize the convective terms in the governing equations. They have used SIMPLE algorithm with line by line ADI method. At the inlet and exit, fully developed boundary condition and at the wall no slip condition is used by them. They have observed that a sharp increase in average static pressure occurs at the section where the fence is located. They have concluded that, at higher Reynolds number, sudden expansion with fence configuration always performs better than the configuration of simple sudden expansion as far as diffuser efficiency is concerned. They have suggested that, for best performance of the diffuser, the position of the fence should be located from the throat, at a non-dimensional distance of around 1 from the throat in the direction of flow in case of higher flow Reynolds number.

Layek et al (2008) have carried out numerical simulation to study the effects of suction and blowing on flow separation in a symmetric sudden expansion channel. They have considered uniform blowing or suction at the lower and upper porous step walls. They have used expansion ratio of 1:2 and non-dimensional inlet channel length of 4. During computation, Reynolds number ranging from 100 to 500 is considered by them. They have used two dimensional continuity and Navier-Stokes equations for the flow of incompressible and viscous fluid. The governing equations are solved by a control volume based finite difference method with staggered grid arrangement which is proposed by Harlow and Welch (1965). During numerical simulation, they have used two level forward time-differencing formula for time derivative terms, hybrid scheme consisting of the central

differencing and the second-order upwind for convective terms, a second-order accurate three-point central difference formula for diffusive terms in the momentum equations. At the inlet and outlet section of the channel, the fully developed flow is considered by them. They have observed that the blowing through the channel wall makes the asymmetric nature of flow to the symmetric by diminishing the region of separation. But the symmetric nature of flow becomes asymmetric by the application of suction from the porous channel wall. They have obtained critical Reynolds number for the flow bifurcation (i.e. flow asymmetry) and this value increases with increase of the blowing speed. They have got critical Reynolds number (for flow symmetry) of about 260, by considering higher blowing speed. Without blowing or suction critical Reynolds number is about 125. They have observed that by the application of blowing, the separation point shifts towards downstream of the channel and the reattachment point towards the upstream direction of the channel. Thus, blowing shrinks the size of the recirculation zone.

Nguyen et al. (2008) have experimentally studied turbulent lean premixed pre-vaporized (LPP) reacting flows behind a double symmetric, plane sudden expansion. In their configuration, they have considered a splitter plate at the inlet region of the sudden expansion placed centrally, so that the inlet channel divides two equal channels (upper and lower channel). The exit of the splitter plate is in convergent shape with 14^{o} inner angle. The trailing edge of the splitter plate is placed certain distance before (upstream) the sudden expansion plane. They have considered Reynolds number of 25,000, based on bulk velocity and height of each inlet channel. Commercial propane is used as fuel. They have performed flame visualizations of the combustion zone just behind the dump plane. To measure velocity, Laser Doppler velocimetry method is used. In the non-combusting case, they have observed that the mean velocity field past the dump plane is asymmetric with the formation of two unequal recirculation zones. They have also seen that the presence of combustion shorten the recirculation zone size and restore the symmetry in the case of the homogeneous reacting flow. They have noted that the values of the equivalence ratio at which the lean extinction of the reaction zones occurs are almost independent from the Reynolds number of the inlet flow.

Tsai et al. (2009) have experimentally investigated the transient cooling process in a sudden-expansion channel with the injection of cold air from the porous bottom wall. They have considered aspect ratio (the ratio of channel width to step height) of 15.4, inlet stream velocity of 3.8 m/s and volume flow rates of the injected air from 0.833×10^{-3} to 5.0×10^{-3}

m^3/s. The images of the flow patterns are recorded by using a high speed motion analyzer (Kodak KTAPRO-TM). Laser- Doppler velocimetry (LDV) system is used by them to measure the average velocity. With respect to the various wall injection rates, four different flow patterns are identified by them. These are the recirculation pattern, the elevated recirculation pattern, the transpiration pattern, and the film pattern. When wall injection is lowest in magnitude the flow is considered by them as recirculation pattern. For the recirculation pattern, they have observed that the reattachment point locates at 5 to 6 times of step height (H). As wall injection increases the flow becomes elevated recirculation pattern. They have observed that the reattachment length (7.7 H) increases for the case of elevated recirculation pattern comparing to the recirculation pattern. Increasing the wall injection transforms the flow into the transpiration pattern. For the transpiration pattern, they have seen that the adverse pressure gradient is no longer sustained, and the recirculation bubble is noticeably lifted and squeezed. Further increasing the wall injection, they have observed film pattern in the flow feature. For film pattern, no noticeable reattachment of the flow is observed by them and the main recirculation vortex is completely destroyed. They have observed that most of the mixing between the heated inlet stream and the injected coolant occurs at the horizontal planar shear layer, except for the flow neighboring the back step.

Ayache et al. (2010) have experimentally and numerically studied the flow characteristics of acoustically forced isothermal air flow through a modified sudden expansion configuration. The upstream region of the sudden expansion consists of two concentric circular ducts with bluff body. The bluff body is of conical shaped (45^o half-angle) and gives a blockage ratio of 50%. The flow upstream of the duct is pulsed by a loudspeaker at a single frequency and with large amplitude. They have considered Reynolds number of 16,000. During experiment, Laser-Doppler Anemometry system is used to measure stream-wise and radial velocities. They have used Large Eddy Simulations with PRECISE code to simulate the flow. PRECISE is a low Mach number, finite-volume code that uses structured grids. For pressure-correction equation, the SIMPLE algorithm (Patankar, 1980) is used by them. Convective transport is discretized by using a second-order central difference scheme, while time derivatives are discretized with a second-order backward difference scheme. At the inlet boundary, they have considered the velocity as monochromatically forced (contains white noise) and uniform across the duct. No-slip velocity conditions are used on solid walls, while at the outlet, zero gradient boundary condition is considered by

them. They have seen that at low forcing frequencies, the recirculation zone is pulsated with the incoming flow, at a phase lag that depends on spatial location. At these frequencies no clear vortex shedding is observed by them. They have noted that at high forcing frequencies, vortices are shed from the bluff body and the recirculation zone, as a whole, is less pulsated. Zohir et al. (2011) have experimentally investigated the heat transfer characteristics and pressure drop for fully developed turbulent air flow in a sudden expansion pipe with downstream modification. They have used a propeller fan (15 blades and $\theta=65^{o}$) and spiral spring as turbulator to produce turbulent swirling flow at the downstream of the sudden expansion. They have used Reynolds number ranging from 7500 to 18500 and pipe expansion (upstream pipe diameter/downstream pipe diameter) in the range of 0.3 to 0.65 under a uniform heat flux condition. During their experiment, surface temperature is measured by using thermocouples of K-type. They have seen that there is a significant effect of Reynolds number on local Nusselt number when the propeller swirl generator is located nearest to the sudden expansion edge at X/H = 1 and this effect decreases with increasing the distance to X/H = 5 and 10. As the Reynolds number increases for a given position of swirl generator, they have observed that the Nusselt number also increases indicating enhanced heat transfer coefficient. The Nusselt number in the swirling flow is higher than that for axial flow in a sudden expansion plain pipe at a fixed value of Reynolds number, which is observed by them. They have noted that the recirculation zone in the swirl flow improves the convective heat transfer.

Banerjee et al. (2011) have numerically studied the performance of a modified sudden expansion diffuser in terms of static pressure rise. In their configuration, they have considered two fences at the downstream of the sudden expansion for fixed fence subtended angle of 10^{o}. They have compared their results with plain sudden expansion configuration. They have considered Reynolds number ranging from 20 to 160 and an aspect ratio of 2. The flow is considered by them as steady, two-dimensional and laminar. During numerical simulation, governing equations are solved by finite difference method. For convective term discretization, they have used power law scheme. SIMPLE algorithm with line by line ADI method is used for pressure velocity coupling. At the wall, no slip boundary condition is used. At the inlet and outlet, they have considered fully developed flow condition. In high Reynolds number regime, they have observed that average static pressure rise is more in case of sudden expansion with two fences or single fence compared to the plain sudden expansion configuration.

Fattah (2012) has experimentally and numerically studied fluid flow and heat transfer characteristics in the case of wall injection besides main flow through a circular sudden enlargement. In his configuration, injected flow is achieved through an annular slot of the vertical side wall. For wall injection, he has considered rectangular slots with different angles placed at the horizontal outer wall of the annular slot. The Reynolds number of injected flow is considered in the range of 320 to 840 and for the case of main flow the Reynolds number is used in the range of 5895 to 8450. He has considered different injection flow angles as 0^o, 15^o, 30^o, 45^o and 60^o. During experimental investigation, he has measured static pressure distribution by using U-tube differential manometer. The volume flow rates for main and injected flow are measured by orifice meter. During numerical study, he has considered two-dimensional, steady, turbulent and incompressible fluid flow with no heat dissipation. He has used continuity equation, axial and radial momentum equations and energy equation to describe mathematical model. To solve the governing equations, finite difference method with staggered grid system is considered by him. He has used SIMPLE algorithm. The convergence is considered, when the mass imbalance is less than 10^{-3}. He has observed that the intensity of secondary flow in recirculation region decreases by increasing the injection flow rate. He has noted that the recirculation zone decreases at higher value of injection flow rate (for constant value of injection flow rate and small value of the main flow). As the injection flow rate increases at constant injection angle ($\theta = 0^o$) and constant main flow rate, the turbulent kinetic energy decreases. As the injection flow angle increases, he has observed that the pressure recovery increases and its maximum value at the reattachment point shifts in upstream direction.

Tsai et al. (2012) have numerically and experimentally investigated the flow characteristics of Newtonian fluid through a sudden expansion microchannel. In their configuration, they have considered a rectangular block structure placed centrally at the downstream of expansion channel at a certain distance away from the sudden expansion plane. They have used Reynolds number ranging from 0 to 465 for an expansion ratio of 3. During their experimental study, particle image velocimetry method is used for velocity measurement and a shutter controllable CCD camera is used for image recording via a high-speed image acquisition interface. For numerical simulation, they have considered incompressible mass and momentum equations in a steady state condition. Finite volume based FLUENT software is used to perform their simulation. They have used first order upwind scheme for the spatial discretization of the convection term of each governing equation. SIMPLE

algorithm is used for pressure and velocity field coupling. The normal residual for convergence criteria is considered lower than 10^{-6}. They have observed that the distance between the sudden expansion plane and the rectangular block affects the size of the corner recirculation for a constant Reynolds number. They have seen that the size of the vortex structure increases as the distance of the block downstream of the expansion channel increases. But the size of the vortex behind the block structure is insensitive to distance. While this distance is long enough, the corner recirculation size is not sensitive to the location of the block structure. Different types of flow structure are observed by them based on the Reynolds number variation. At low Reynolds number no visible recirculation formed downstream of the expansion channel and this flow structure is termed by them as no recirculation. As Reynolds number increases (Re 100), the inertial effects results in the development of recirculation lip vortices and this flow structure is termed as lip recirculation. At Re 265, they have observed that the recirculation grows with the fluid inertia and extends to the side wall.

Kim and Santavicca (2013) have experimentally studied the combustion instability mechanisms induced by convective/acoustic wave interferences in a model lean-premixed swirl-stabilized gas turbine combustor with modified dump configuration. At the inlet zone of the dump plane, they have considered a mixing chamber with a center body which forms an annular cross section. A 300 flat-vane axial swirler with 6 vanes is mounted in the mixing tube. The area expansion ratio from the nozzle to the combustion chamber is used approximately 8.2. An ICCD camera (Princeton Instruments model 576G) is used to record the flame images. They have measured temporal variations of equivalence ratio at the combustor inlet using the infrared (IR) laser absorption technique. They have observed that the forced flame dynamics are characterized by the strong interaction between the 'ring-shaped' reaction zone in the corner recirculation zone and the primary reaction zone stabilized at the inner shear layer.

Ali-Baig and Khan (2012) have experimentally studied the effect of different levels of over expansion on base pressure in a suddenly expanded axisymmetric duct. At the inlet to the sudden expansion geometry, they have considered a convergent-divergent nozzle. At the exit periphery of the nozzle, blowing is considered by them on the vertical wall. They have conducted experiment for Mach numbers 2.2 and 2.58 at a fixed level of over expansion of 0.277 and 0.56. Ares ratio of 3.24 and L/D (Exit length/diameter of sudden expansion) ratio in the range of 1 to 10 are used by them. They have observed that the maximum gain in the

base pressure at Mach number 2.2 is around 60 percent when the level of over expansion is changed from 0.277 to 0.56. For the same variation of over expansion, base pressure gain is around 70 percent at Mach 2.58. They have seen that the minimum duct length required for Mach numbers 2.2 and 2.58 are L/D = 6 for a level of over expansion of 0.277. When the level of over expansion is 0.56, minimum L/D ratio required for Mach numbers 2.2 and 2.58 are 3 and 4 respectively.

Tuncer et al. (2014) have experimentally investigated the stability and structure of lean premixed methane air flames in a swirl stabilized premixed dump combustor at atmospheric pressure. At the inlet of the dump plane, they have considered a 450 angled eight blades swirl vane which is installed on a 20 mm diameter center body. For measurement of the structure of the cold flow, particle image velocimetry (PIV) technique is used by them in order to gain useful insight into the flow field. A CCD camera with 1200 × 1600 pixels resolution is used for imaging. They have studied the flow field for fixed Reynolds number of 19400 with a constant swirl number of 0.74. They have observed two elliptically shaped counter rotating recirculation vortices behind the dump plane and a central recirculation zone just downstream of dump plane. They have noted that the swirling flame is neatly stabilized above the dump plane. Furthermore, this flame structure is slightly asymmetric.

Saha and S. Chakrabarti (2016) have numerically examined the impact of Reynolds number on the ferromagnetic liquid with considered MHD phenomenon. They have numerically investigated two dimensional, incompressible, Newtonian and electrically conducting laminar fluid flow characteristics considering the MHD phenomenon. A water base magnetic fluid, flowing through a channel under the action of magnetic field, had been chosen and applied along axial direction. The continuity and momentum equations, considering laminar and Magneto hydro dynamics (MHD) are solved for magnetic number arising from MHD of 3.66 and for Reynolds numbers ranging from 80 to 200. They concluded that the flow characteristics such as stream line contour, vorticity magnitude contour, tangential velocity contour, wall static pressure, and wall shear stresses, which are thoroughly investigated, have a higher importance in case of various industrial applications such as diffuser, heat exchanger, combustion chamber, industrial equipment, processing plants.

Mandal et al. (2017) have numerically examined the performances of a rapid expansion dump combustor by inserting restrictions around the throat region in order to understand the fluid dynamics phenomena by incorporating different types of restriction or alteration

in geometry. They have contrasted their model with three restricted, straightforward expansion designs for low Reynolds numbers of 1.2×10^5 and aspect ratio of 2 and central restriction of 100%. Their work concluded that more recirculating bubbles are formed for a modified dump combustor than plain dump combustor. Also among the modified dump combustors, combustor with fillet shaped restriction has better performance in terms of chamber mixing.

S. Saha and S. Chakrabarti (2020) have examined the 2D turbulent flow subjected to a magnetic field, coursing through a square shape Channel. The impact of Magnetic number arising from Magneto Hydro Dynamics (MHD for a fixed Reynolds number on the flow characteristics has been presented in detail in their investigation. They have shown that the flow parameters like wall shear and pressure of wall are increased with increasing Magnetic number and the number of recirculating bubbles increases with decreasing in Magnetic number. They have concluded that the formation of the recirculating zone increases the retention time of fluid which results in the enhancement of heat transfer for a specific surface of a heat exchanger.

In this numerical study, an attempt has been made to analyze the fluid flow characteristics in a simple annular dump combustor and modified dump combustors with certain central restrictions like rectangular and spherical shape. Flow characteristics and patterns are depicted sequentially in terms of streamlined contours, axial velocity profile, and the centerline velocity profiles in the result and discussion section. The above-mentioned flow characteristics are studied at several locations in the flow field with Reynolds numbers ranging from 10^3 to 10^6 for different models. The governing two-dimensional partial differential equations for conservation of mass and momentum are discretized with the help of the control volume-based finite volume method. The discretized equations are solved iteratively by SIMPLE algorithm with the help of second order upwind scheme for a fixed aspect ratio of 3 and central restriction of 120%. From the numerical investigation, it has been seen that the number of formations of a recirculating bubble increases with increasing Reynolds number. The formation of bubbles has immense importance in case of mixing in ship combustors. It can be mentioned that more recirculating zones ensure desirable mixing of fluids in ship combustor and helps significantly in the reduction of temperature, NOX emission, and combustion residuals. In order to authenticate the present numerical simulation, a validation is performed in terms of axial velocity and presented in the sub-section of Mathematical formulation.

CHAPTER-2

MATHEMATICAL FORMULATIONS

2.1 Computational domain:

Schematic diagrams of the computational domain for turbulent flow through a rigid asymmetric annular dump combustor and modified annular dump combustor with various central restrictions are presented in figure 1, 2, 3, 4 and 5 respectively. The external dimensions of the simple dump combustor are taken from Mandal et al. (2017). For the modified geometrical modelling of dump combustor, inlet length throat and combustor casing length are taken as 0.08 m and 0.3 m respectively. The inlet manifold radius and outlet manifold radius are taken as 0.02 m and 0.06 m respectively. The diameter and length of the central restriction are considered as 0.048 m and 0.06 m respectively. For figure 3 and 4, the radius of the circular arc is taken as 0.024 m.

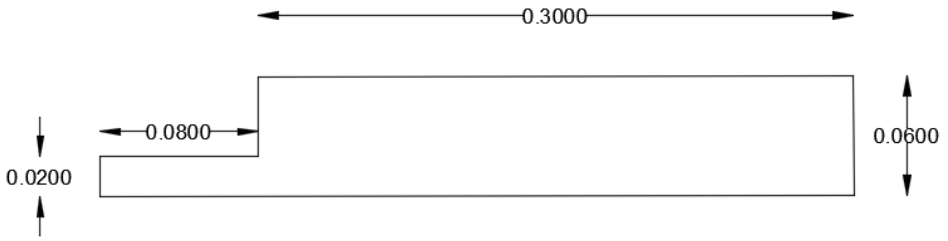

Figure 1. Computational domain of simple dump combustor without any restriction.

The flow is considered as two dimensional, turbulent and symmetric about axis. The fluid is assumed to be incompressible and follows Newtonian laws.

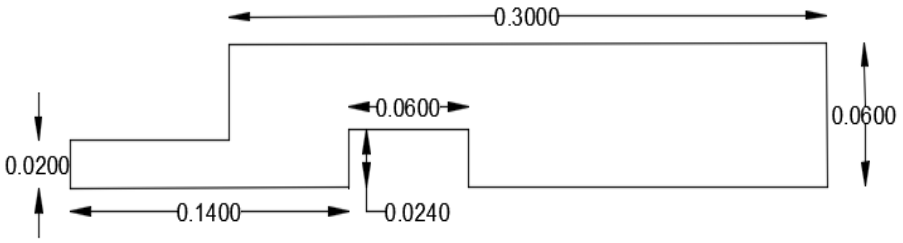

Figure 2. Computational domain of modified dump combustor with rectangular cavity.

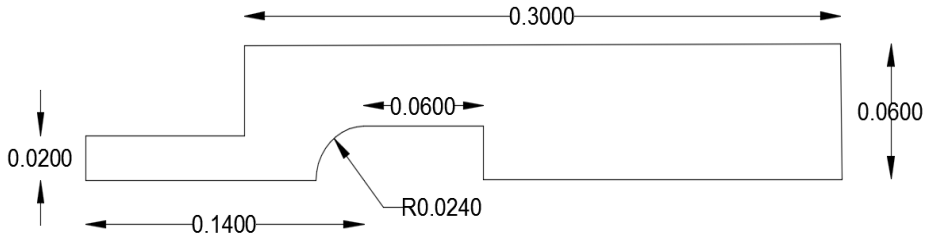

Figure 3. Computational domain of modified dump combustor with rectangular curved cavity.

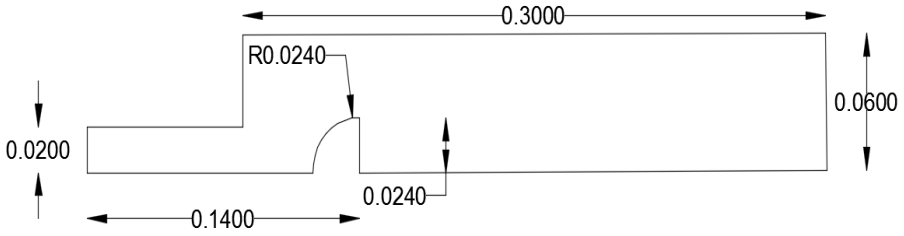

Figure 4. Computational domain of modified dump combustor with semi- hemispherical cavity.

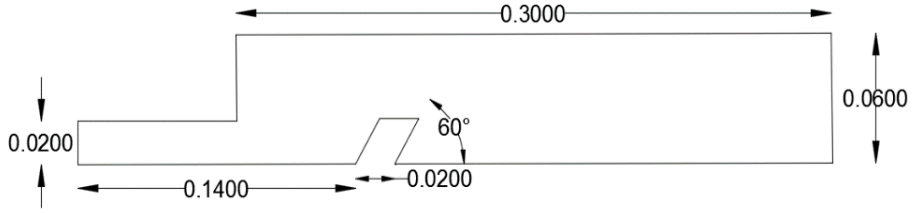

Figure 5. Computational domain of modified dump combustor with diagonal cavity.

2.2 Governing Equations for Turbulent Flow:

Continuity equation: $\frac{\partial u}{\partial x}+\frac{\partial v}{\partial y}=0$…….…… (1)

Momentum equation in X-axis: $\rho\left(u\frac{\partial v}{\partial x}+v\frac{\partial u}{\partial y}\right)=-\frac{\partial p}{\partial x}+\frac{\partial \tau_x}{\partial x}$……..... (2)

Where, τ_x is the turbulent stress tensor along x direction and,

$\tau_x=\left[\mu\left(\frac{\partial u}{\partial x}+\frac{\partial u}{\partial y}\right)\right]-\frac{2}{3}\mu\frac{\partial u}{\partial x}]$

Momentum equation in Y-axis: $\rho\left(u\frac{\partial v}{\partial x}+v\frac{\partial y}{\partial y}\right)=-\frac{\partial p}{\partial y}+\frac{\partial \tau_y}{\partial y}$…… (3)

Where,τ_y is the turbulent stress tensor along y direction and $\tau_y=\left[\mu\left(\frac{\partial v}{\partial x}+\frac{\partial v}{\partial y}\right)\right]-\frac{2}{3}\mu\frac{\partial v}{\partial y}$

The governing realizable k-**ε** equations representing the turbulent flow properties are as below.

k- Equation: $\rho\left(\mathrm{u}\frac{\partial \mathrm{k}}{\partial \mathrm{x}}+\mathrm{v}\frac{\partial \mathrm{k}}{\partial \mathrm{y}}\right)=\frac{\partial}{\partial \mathrm{x}}\left[\left(\mu+\frac{\mu_t}{\sigma_k}\right)\frac{\partial \mathrm{k}}{\partial \mathrm{x}}+\left(\mu+\frac{\mu_t}{\sigma_k}\right)-\frac{\partial \mathrm{k}}{\partial \mathrm{y}}\right]+\rho\mathrm{G}-\rho\boldsymbol{\varepsilon}$

ε- Equation: $\rho\left(\mathrm{u}\frac{\partial \varepsilon}{\partial \mathrm{x}}+\mathrm{v}\frac{\partial \varepsilon}{\partial \mathrm{y}}\right)=\frac{\partial}{\partial \mathrm{x}}\left[\left(\mu+\frac{\mu_t}{\sigma_\varepsilon}\right)\frac{\partial \varepsilon}{\partial \mathrm{x}}+\left(\mu+\frac{\mu_t}{\sigma_\varepsilon}\right)-\frac{\partial \varepsilon}{\partial \mathrm{y}}\right]+\rho\mathrm{C1S}\boldsymbol{\varepsilon}+\mathrm{C1}\boldsymbol{\varepsilon}\frac{\varepsilon}{k}\ \mathrm{C3}\boldsymbol{\varepsilon}\mathrm{G}-\rho\mathrm{C2}\ \frac{\varepsilon^2}{k+\sqrt{v\varepsilon}}$

Where, G is the production term and it represents the transfer of kinetic energy from mean flow to turbulent motion through the interaction between the turbulent fluctuations and the mean flow velocity gradients, **ε** is the rate of dissipation of turbulent kinetic energy due to viscous effects. The turbulent viscosity considered for the simulation is given by, $\mu_t = \rho C_\mu \frac{k^2}{\varepsilon}$.

Here,C_{mu}, $C_{1\varepsilon}$, and $C_{2\varepsilon}$ are the turbulent constants. The values are taken according to the standard k-**ε** model along with standard wall functions. The values of $C_{mu}, C_{1\varepsilon}, C_{2\varepsilon}$ are considered as 0.09, 1.44, and 1.92 respectively. These values of turbulent constants are taken from Launder and Spalding (1974).

2.3 Boundary Conditions:

The following boundary conditions have been chosen for the present analysis:

- At walls: No slip condition, i.e. velocity component near wall is zero.
- At inlet: Axial velocity is specified and transverse velocity is taken as zero,$i.e., u = \frac{R_e \mu}{\rho d}, v = 0\ and\ \mathrm{P_{d-in}} = \frac{\rho {u_i}^2}{2}$
- At outlet: Constant pressure has been considered, i.e. gauge pressure is zero.
- At axis: The normal gradient of axial velocity and transverse velocity are set as zero.

2.4 Numerical Methodology:

The dimensional partial differential continuity and momentum equations (1), (2) and (3) have been solved according to the SIMPLE method in the finite volume formulation by the use of a uniform grid in both coordinating directions. The convection and diffusion terms have been discretised with the help of second order upwind scheme. The discretized equations have been solved iteratively by using line-by-line ADI (Alternating directional

implicit) method. The turbulent k-$\mathcal{E}$ viscous model has been selected for simulation. For all calculations, the length, inlet and outlet radius of the axisymmetric dump combustor are considered to be 0.38 m, 0.02 m and 0.06 m respectively For this simulation the value of μ and ρ are considered to be 1.7894×10^{5} Ns/m^2 and 1.225 kg/m^3 respectively. Inlet velocity is obtained by equation the value of Reynolds number in the relation, Re = $\frac{\rho u_i D_i}{\mu}$. The dynamic pressure inlet is obtained by using the relation, $P_{d\text{-}in} = \frac{\rho {u_i}^2}{2}$, where u_i is the inlet velocity. The gauge pressure at combustor outlet is taken as zero. At the instant of time, when the normalized residuals for mass and momentum equations, summed over the entire calculation domain during computations, fall below 10^{-4}, the convergence of the iterative scheme is assumed to be achieved.

2.5 Validation:

In order to authenticate the present numerical investigation, a validation has been carried out in terms of axial velocity by comparing the numerical present work with the work presented by the Mandal et al. (2017) in their simulation.

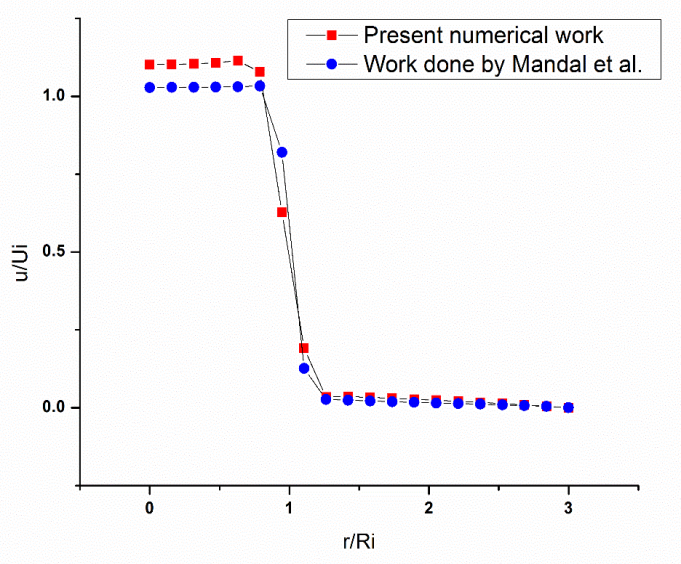

Figure 6. Axial velocity profile of the present work and the work presented by Mandal at al. (2017)

Validation has been performed on simple dump combustor with aspect ratio 3 and Reynolds number 10^5. The same has been presented in the figure 6. From the figure 6 it has been observed that, the distribution of the axial velocity profiles of present work and the work done by the above mentioned researcher are shown excellent agreement in terms of both quality and quantity.

CHAPTER-3

RESULTS AND DISCUSSION:

The results of the present study are presented in this section. The parameters chosen for this study are as follows:

- Reynolds number, Re = 10^3, 10^4, 10^5, and 10^6.
- Aspect Ratio (AR) is taken as 3.
- Central restriction's radius with respect to inlet manifold is 120%.
- Dump combustor dimensions are taken from Mandal et al. (2017).

3.1 Study of Streamline Contours:

The families of curves known as stream lines are immediately tangent to the flow's velocity vectors. The streamline contour graphs illustrate how the recirculating zone is affected by Reynolds number for different aspect ratios (AR). For varied shapes of central limitation and fixed AR, four different Reynolds numbers, 10^3, 10^4, 10^5, and 10^6 are taken into consideration. This research demonstrates that the flow through an annular dump combustion chamber is composed of two primary components: a high velocity flow in the geometry's center and sluggish recirculation bubbles towards the cavity. All types have a similar high velocity area, however the recirculating portion differs depending on the restriction setup.

The disrupted flow conditions may significantly alter the pressure gradient inside the combustor casing and alter the fluid's velocity, both of which contribute to effective fluid mixing.

3.1.1 Stream line contours for simple dump combustor:

Figure 7 shows turbulent flow for a simple dump combustor for aspect ratio 3. At Re = 10^3 there is formation of recirculating zone at the throat and near top left corner of combustor casing. The fluid exits at high velocity due to the fact that recirculating zone is concentrated towards the inlet region inside the simple combustor. As the value of Reynolds number is increased to 10^5 and 10^6 the size of recirculating zone is enlarged covering the entire top half of axisymmetric combustor casing, it also shifts towards outlet where the fluid bubbles are in a vortex field and hence exit with velocity comparatively lesser than compared to low

Re. However there is proper mixing observed at fluid's high Reynolds number.

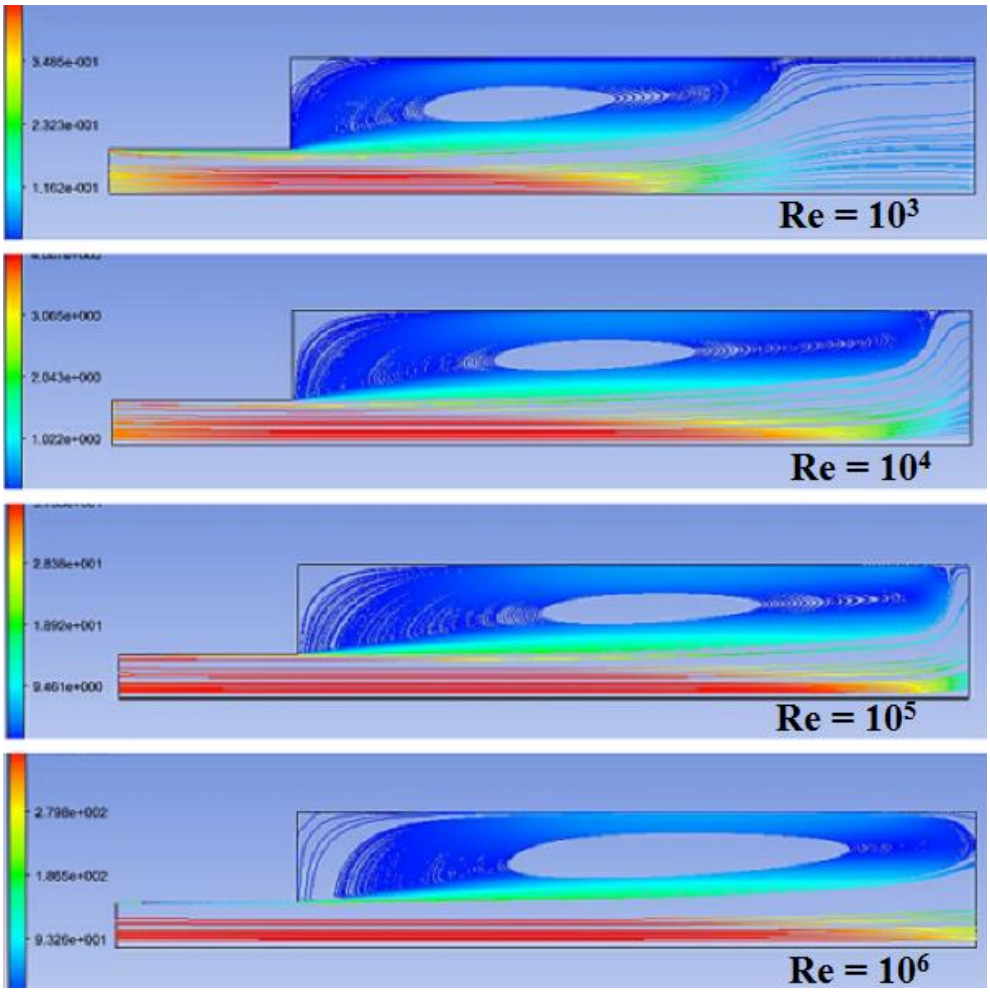

Figure 7. Streamline contour comparison of simple dump combustor for different Reynolds number.

The simple dump combustor's design was taken as reference model and the turbulent results of streamlines agrees with results by Mandal et al. (2017), considering Reynolds number as 1.2×10^5.

3.1.2 Stream line contours for dump combustor with rectangular restriction:

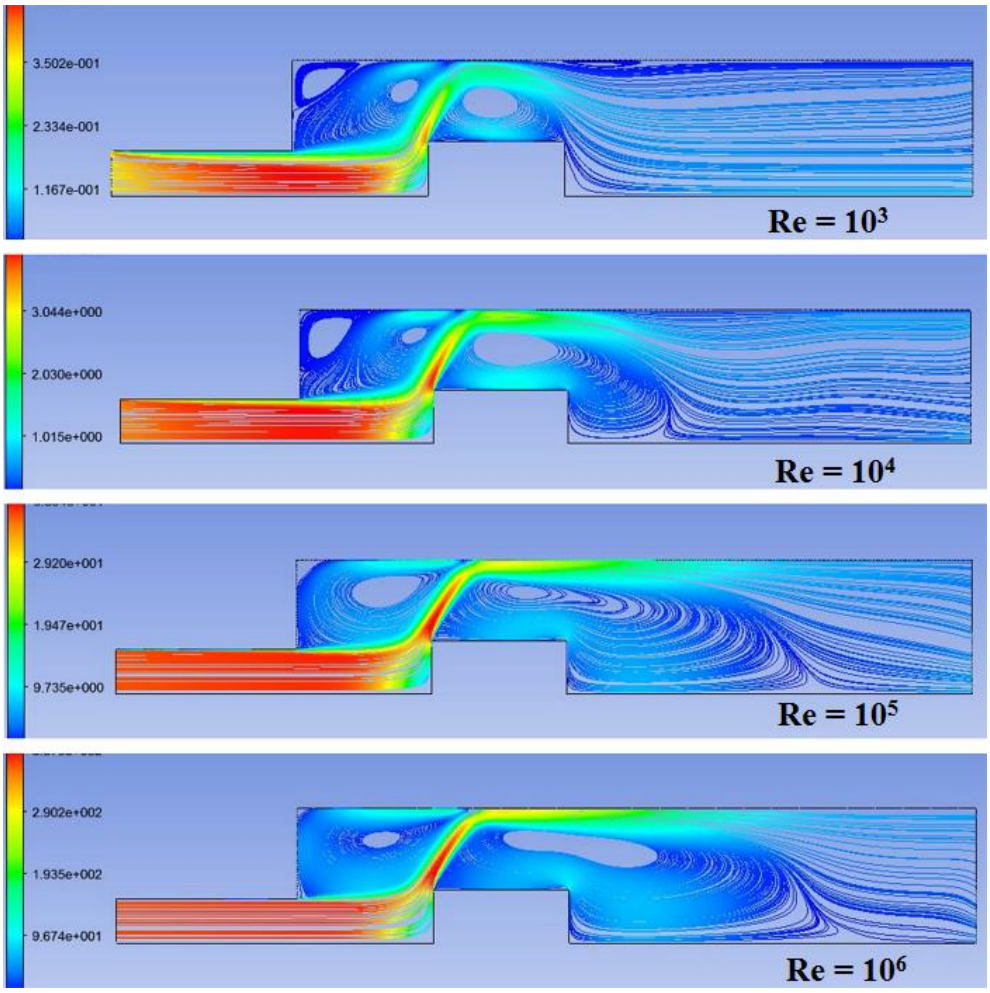

Figure 8. Streamline contour comparison of dump combustor with rectangular restriction for different Reynolds number.

Figure 8 shows the streamline contour of a modified dump combustor with rectangular restriction at distance of 0.14 m from the inlet manifold. The width of restriction is same as outlet radius (0.06 m) and height is 1.2 times of the inlet radius (0.02 m). When Re is 10^3 and 10^4, there is visible corner mixing and central mixing of fluid near the restriction, whereas there is an overall increment in central recirculating zone when Re is 10^6 and presence of large corner mixing zone which is formed as secondary recirculating zones merge together. At Re 10^6 the CRZ is enlarged and covers the entire central combustor casing region after the restriction ends, from x = 2 m onwards.

3.1.3 Stream line contours for dump combustor with rectangular curved restriction:

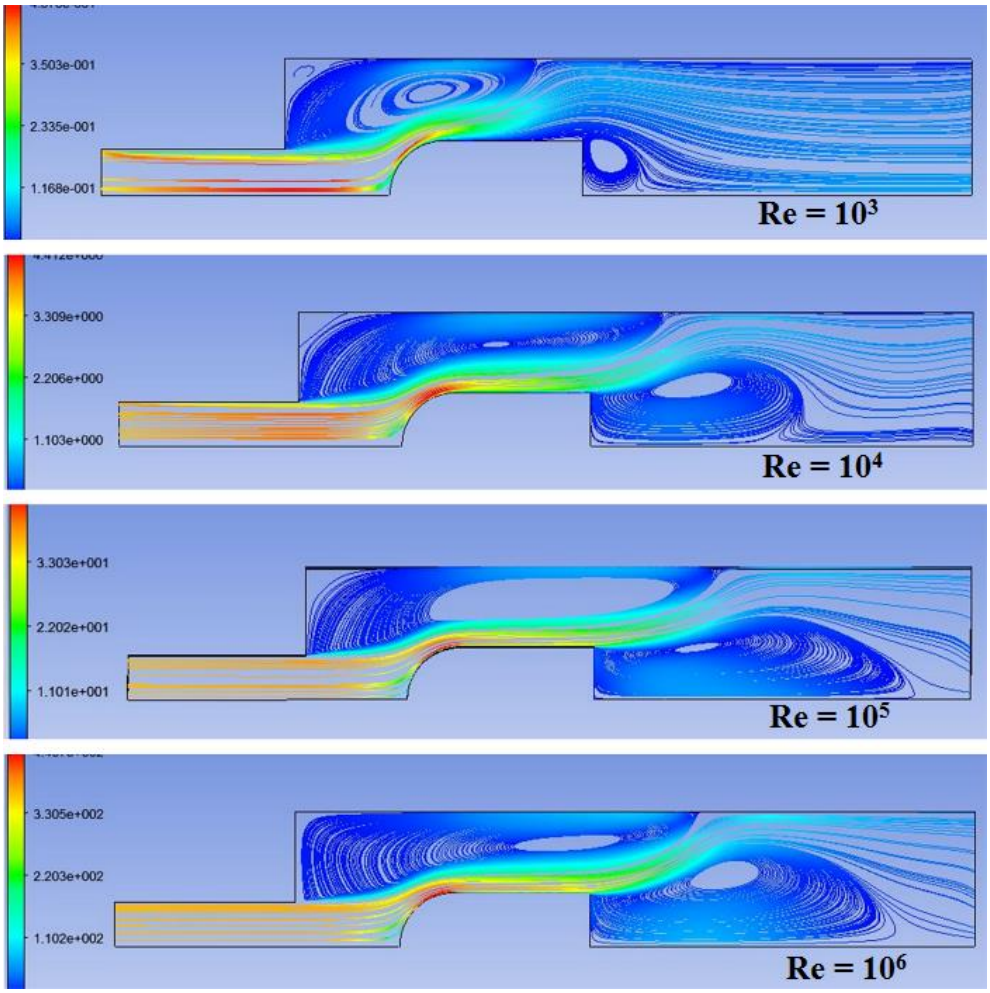

Figure 9. Streamline contour comparison of dump combustor with rectangular curved restriction for different Reynolds numbers.

Figure 9 depicts the effect of Reynolds number on streamline contour when the restriction's shape is a curved at the beginning, unlike in previous model where restriction had sharp edge. It is noticed that streamline contour shows minimum central region mixing at low value of Reynolds number, whereas when Re is increased, rectangular restriction with added front fillet reveals enhanced central mixing of fluid. There is potentially no fluid flow at corner above the throat at low value of Reynolds number, whereas as it is increased 1000 times, there is uniform distribution of CRZ all around the restriction, indicating proper mixing of combustion fluids and low probability of combustion residuals.

3.1.4 Stream line contours for dump combustor with semi-hemispherical restriction:

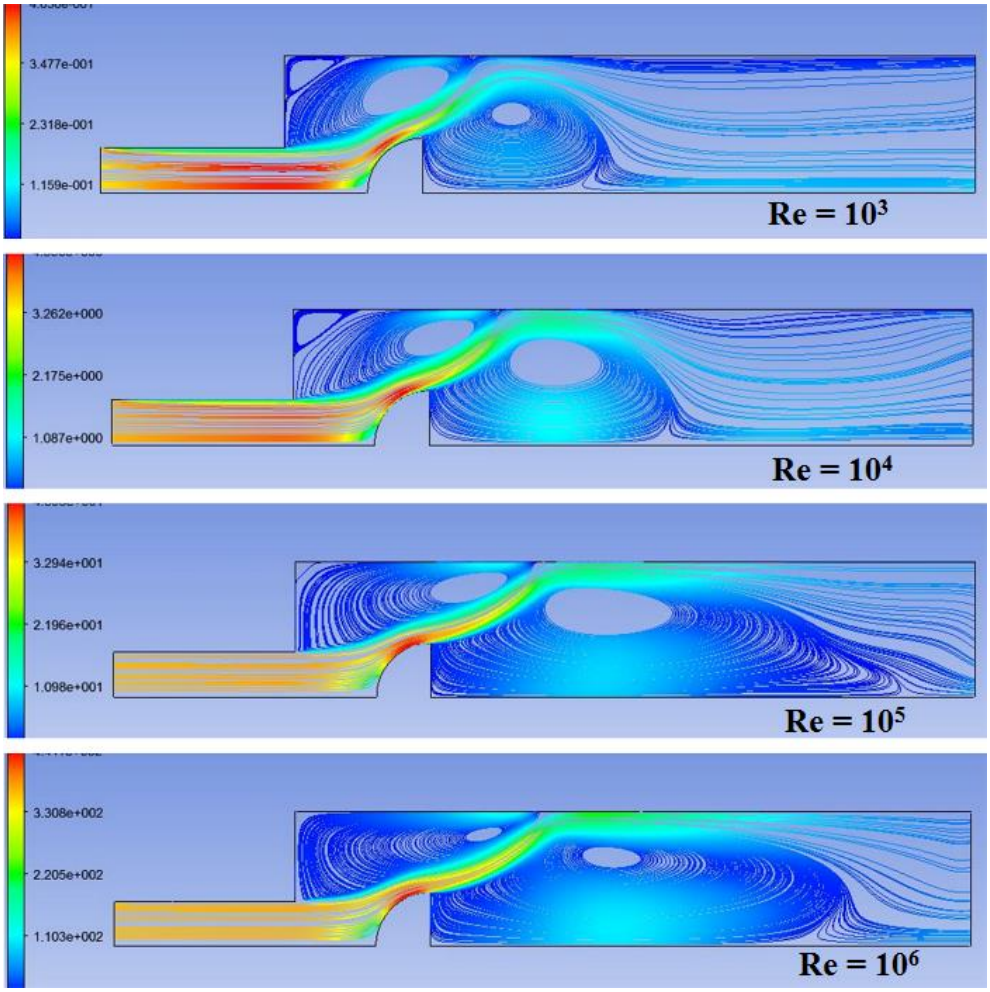

Figure 10. Streamline contour comparison of dump combustor with semi hemispherical restriction for different Reynolds number.

Figure 10 of stream line contour is for spherical restriction which also has a radius of 0.024 m. There is considerable corner mixing and presence of recirculating around the restriction in the above streamline contour of axisymmetric dump combustor with spherical restriction. Also as the value is increased to 10^6, it is noted that the area of CRZ is enlarged and affects the mixing around and before the outlet manifold.

3.1.5 Stream line contours for dump combustor with diagonal restriction:

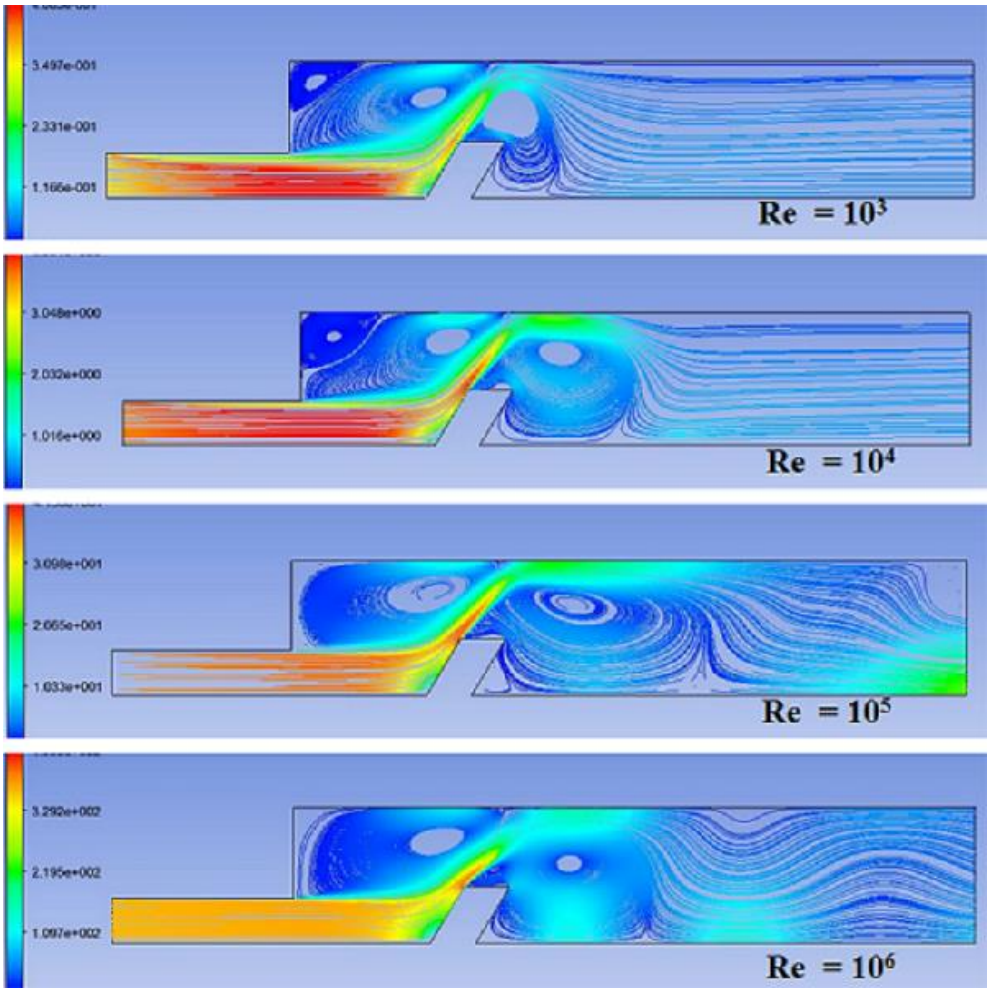

Figure 11. Streamline contour comparison of dump combustor with diagonal restriction for different Reynolds number.

Figure 11 reveals the streamline contour variation on a diagonal shaped central restriction placed at 0.14 m from the inlet manifold and of height 1.2 times of inlet radius. The shape of the restriction, apart from the value of Reynolds number, is the key factor that effects the streamline contours and helps us measure the fluctuation and concentration of recirculating zones within the combustor casing.

3.2 Variation of axial velocity profiles for different value of Reynolds number:

Simple dump combustor and other model of dump combustor with restriction have been studied with respect to axial velocities at x = 0.1 m, 0.14 m, 0.18 m, and 0.22 m respectively. Except for geometry having curved and semi-hemispherical restriction, other models have restriction placed only after a distance of 0.14 m. The values of x axis and y axis in the consequent graphs have been made dimensionless for easy understanding. Corresponding axial velocity graphs for each dump combustor have been studied discussed below.

3.2.1 Simple dump combustor.

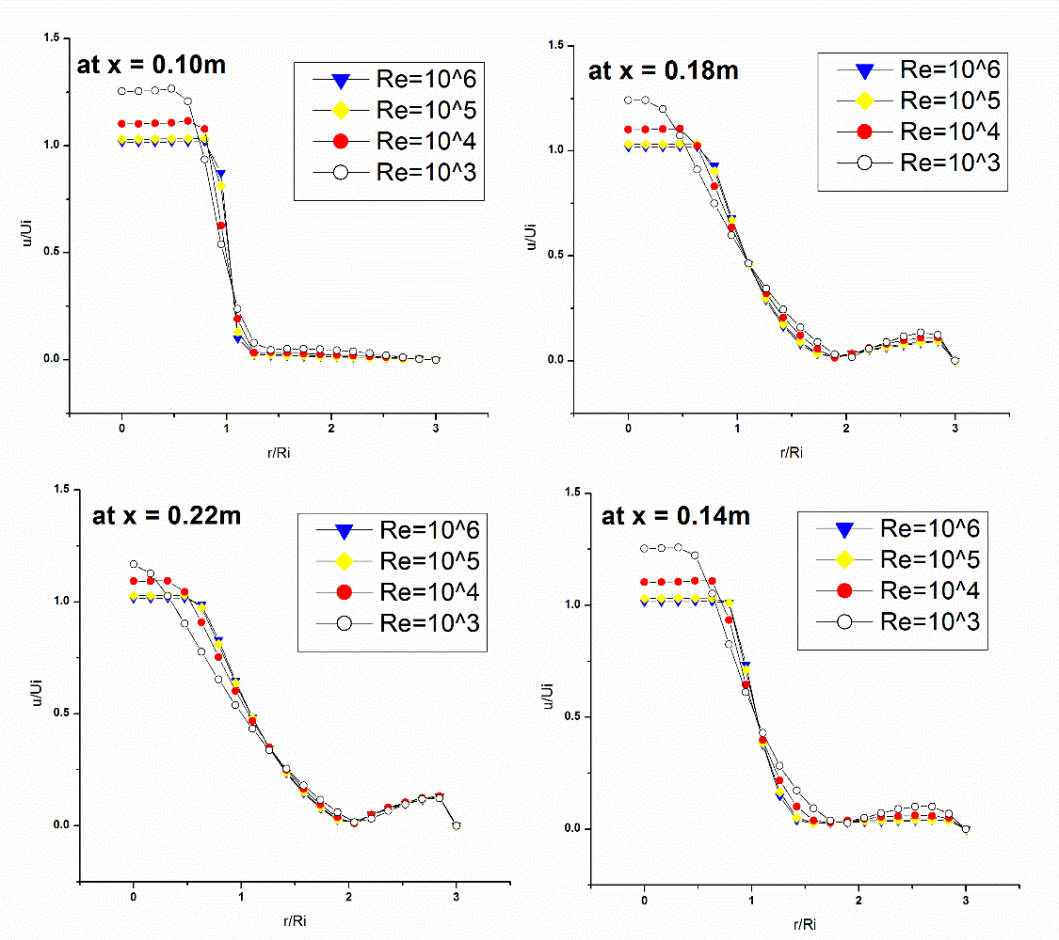

Figure 12. Variation of axial velocity profiles at different axial positions on x- axis for a simple dump combustor.

Figure 12 depicts the variation of an axial velocity profile for a simple dump combustor at different locations along the length of the combustor, such as 0.10 m, 0.14 m, 0.18 m, and 0.22 m respectively. For all the cases, the magnitude of the velocity is smoothly decreased from the axis towards the wall of the combustor and becomes lowest at a specific height, and then starts increasing again towards outlet. Moreover, it gains its highest value at a

particular height well above the centerline and then becomes zero at the wall of the simple dump combustor. The sudden expansion configuration of the dump combustor may be the cause for the above-mentioned observations.

3.2.2 Dump combustor with rectangular restriction.

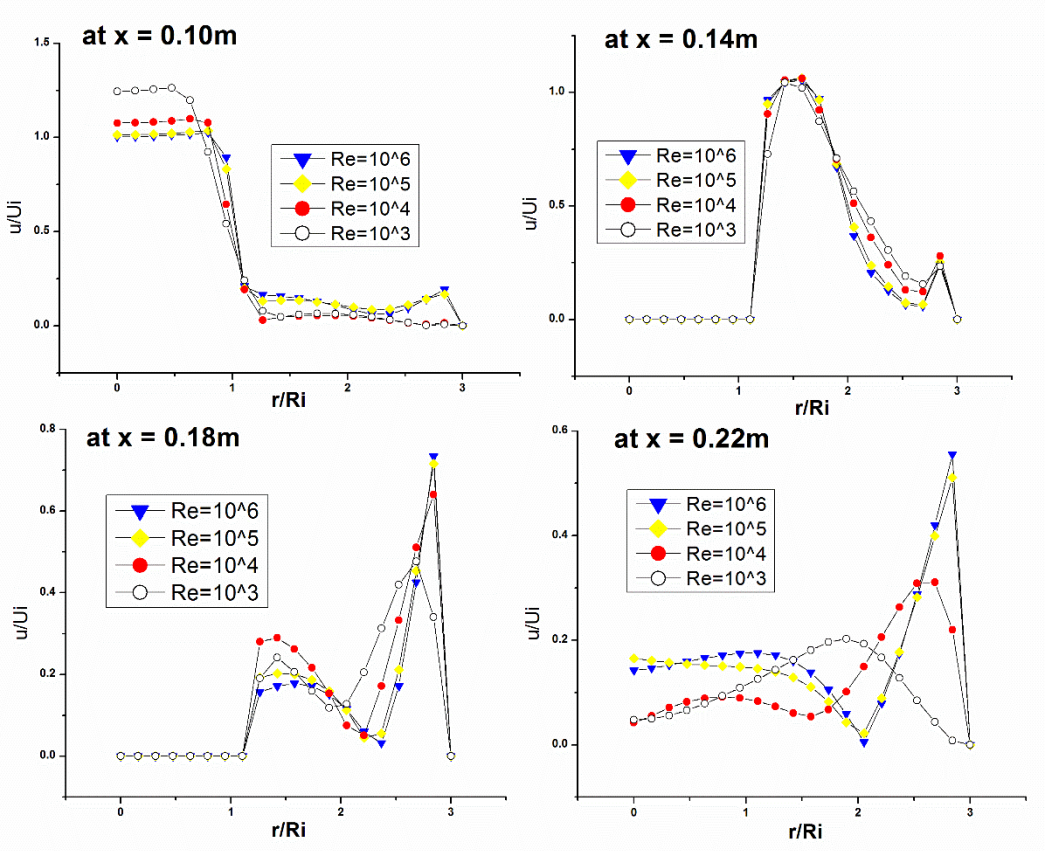

Figure 13. Variation of axial velocity profiles at different axial positions on x- axis for dump combustor with rectangular cavity.

As the geometry of figure 1 is modified to figure 2 by introducing a rectangular restriction on the central axis of the combustor, the variation of axial velocities is obtained as presented in figure 13. From the figure, it has been observed that for the axial location of 0.10 m the axial velocity gains its maximum value at the centerline of the axisymmetric dump combustor as expected and then it is smoothly increased little bit up to a certain height from centerline. After that the magnitude of axial velocity is sharply decreased up to $^{r}/_{R_i}$ of 1.2 for all considered Reynolds number. It has also been seen that in case of Reynolds numbers 10^3 and 10^4, the same is decreased towards the upper wall. Sudden expansion configuration of the combustor may be the probable reason behind this observation.

In case of Reynolds number 10^5 and 10^6, the magnitude of the axial velocity decreases up

to a certain height and after that the same is increased first and then decreased to zero at the wall. The presence of the restriction just after the axial location (x = 0.10 m) may be the cause for the variation. For axial location of 0.14m, it has been clearly seen that the magnitude of axial velocity is found zero up to $^{r}/_{R_i}$ of 1.2, due to presence of front wall of the restriction, thereafter it attains its maximum value due to reduction of sectional area of combustor and then axial velocity starts to decrease smoothly up to a certain height of $^{r}/_{R_i}$ of 2.5, then increases a bit, finally becoming zero at the top wall of the combustor. This velocity flow pattern may be due to presence of rectangular restriction at axial location of 0.14 m. From figure 9, it has also been noted that for axial location of 0.18m, the axial velocity up to $^{r}/_{R_i}$ of 1.2 is zero, thereafter a little rise in velocity is observed, which falls sharply and attains its peak value just near the top wall and becomes zero at the top wall. This may be accounted due to no slip condition at the wall. The flow pattern at axial location 0.18 m may be due to presence of rectangular restriction up to $^{r}/_{R_i}$ of 1.2. Also for axial location of 0.22 m, the axial velocity for Reynolds numbers 103 and 104 consequently increases along the y direction. The same gain its maximum magnitude and then becomes zero at $^{r}/_{R_i}$ of 3. Also in case of Reynolds number 10^5 and 10^6, the magnitude of velocity increases for a bit and then becomes zero at $^{r}/_{R_i}$ of 2. Thereafter it again attains maximum value just near the top wall and becomes zero again at $^{r}/_{R_i}$ of 3. It is observed that there is a significant rise in axial velocity for the axial location 0.22 m. The formation of recirculating bubbles just after restriction may be the cause for the above variation.

The fact that there is a rise in upstream velocity and consequent fluctuation in magnitude of axial velocity after the restriction may be linked to the restriction's configuration and could be considered a cause for the above-mentioned observations.

3.2.3 Dump combustor with rectangular curved restriction.

The distribution of axial velocity for dump combustor with a rectangular curved restriction is presented in figure 14. From the figure, it has been observed that, for the axial location of 0.10 m the axial velocity gains its maximum value at the centerline of the axisymmetric dump combustor. It has also been seen that, in case of Reynolds numbers 10^3 and 10^4, the same is decreased towards the upper wall.

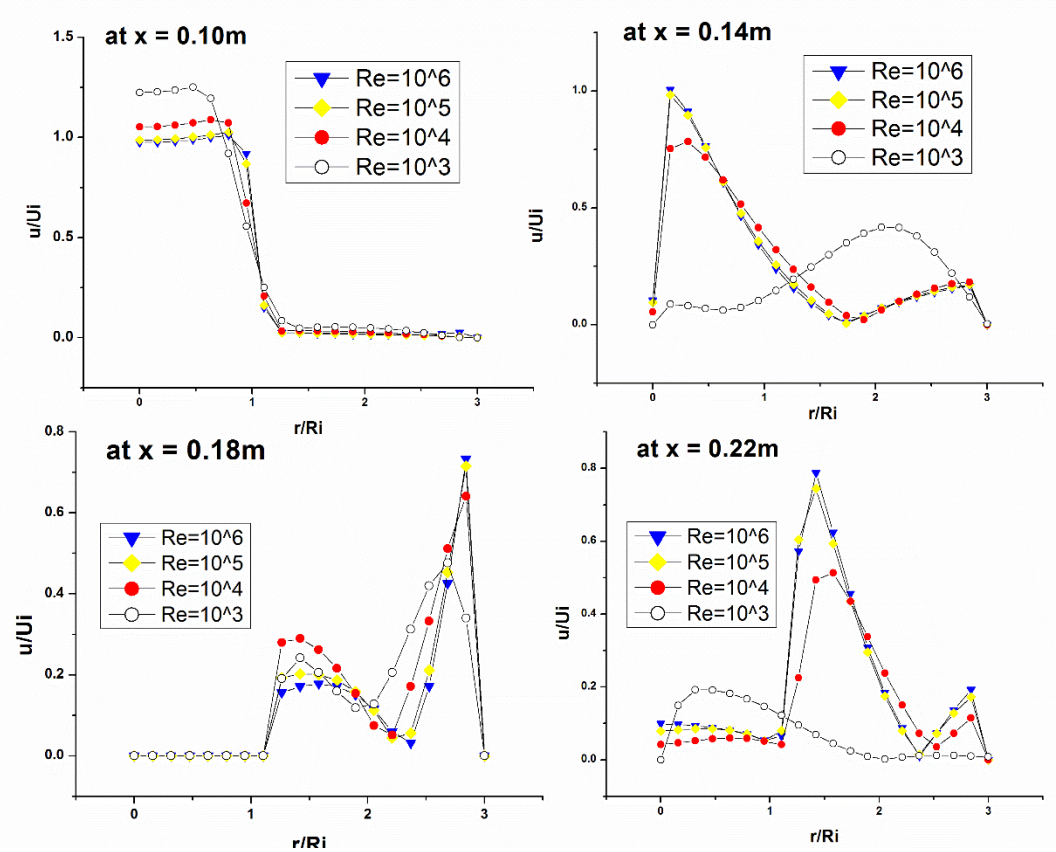

Figure 14. Variation of axial velocity profiles at different axial positions on x- axis for dump combustor with rectangular curved restriction.

In case of Reynolds number 10^5 and 10^6, the magnitude of the axial velocity decreases up to a certain height and after that the same is increased first and then decreased to zero at the wall. The presence of the restriction just after the axial location (x = 0.10 m) may be the cause for the variation. For the axial location of 0.14 m, it has been clearly seen that the magnitude of axial velocity increases sharply up to a certain height for the Reynolds number 10^4, 10^5, and 10^6. It is then noted to sharply decrease and become zero just before $^r/_{R_i}$ of 2. After that it increases again a little and becomes zero near the top wall. In case of Reynolds number 10^3, axial velocity at x = 0.14 m increases at first, then decreases a bit just before $^r/_{R_i}$ of 1. After that the value of axial velocity gradually starts increasing up to $^r/_{R_i}$ of 2, where it attains its maximum value and finally start decreasing until it becomes zero near the top wall. This observation also may be due to presence of front curved wall of the restriction. From figure 14, it has also been noted that for axial location of 0.18 m, the axial velocity up to $^r/_{R_i}$ of 1.2 is zero, thereafter a little rise in velocity is observed, which falls sharply after $^r/_{R_i}$ of 1.5 and it becomes zero at around $^r/_{R_i}$ of 2. It then again increases and

attains its peak value just near the top wall and becomes zero at the upper wall. This may be accounted due to no slip condition at the wall. The flow pattern at axial location 0.18 m may be due to presence of rectangular curved restriction. Also for Reynolds number of 10^3 and 10^4, the value of axial velocity is zero only up to $^r/_{R_i}$ of 1.2 and at the top wall. For axial location of 0.22 m, the magnitude of axial velocity for Reynolds numbers 10^3 increases at first up to $^r/_{R_i}$ of 0.5, attains its maximum value and then smoothly decreases along the y direction till $^r/_{R_i}$ of 2. Thereafter the magnitude remains zero in between $^r/_{R_i}$ of 2 and $^r/_{R_i}$ of 3, i.e., top wall. From figure 14, it can also be said that, the magnitude of axial velocity for Reynolds number 10^4, 10^5, and 10^6 starts decreasing and becomes zero due to presence of restriction wall. It then gains velocity and attains its peak value at $^r/_{R_i}$ of 1.5 and starts decreasing sharply up to $^r/_{R_i}$ of around 2.4. Finally a small gain of velocity (up to $^u/_{U_i}$ of 0.2) is observed after $^r/_{R_i}$ of 2.5 which finally tends to approach zero velocity near top wall of the combustor. The formation of more number of recirculating bubbles just after restriction and the geometry of the restriction may be the probable cause for the above reported variation in axial velocity profiles.

3.2.4 Dump combustor with spherical restriction.

Figure 15 depicts the variation of axial velocity for a dump combustor with spherical restriction. All the curves show that axial velocity for Reynolds number 10^6 and 10^5 has its maximum value near the top wall of dump combustor, than compared to Reynolds number 10^3 and 10^4. For axial location of 0.10 m, it is seen that the axial velocity first increases sharply up to $^r/_{R_i}$ of 0.5, reaches its maximum magnitude and then the curve smoothly decreases up to $^r/_{R_i}$ of 2, thereafter it gains little momentum and finally attains zero velocity at top of the wall.

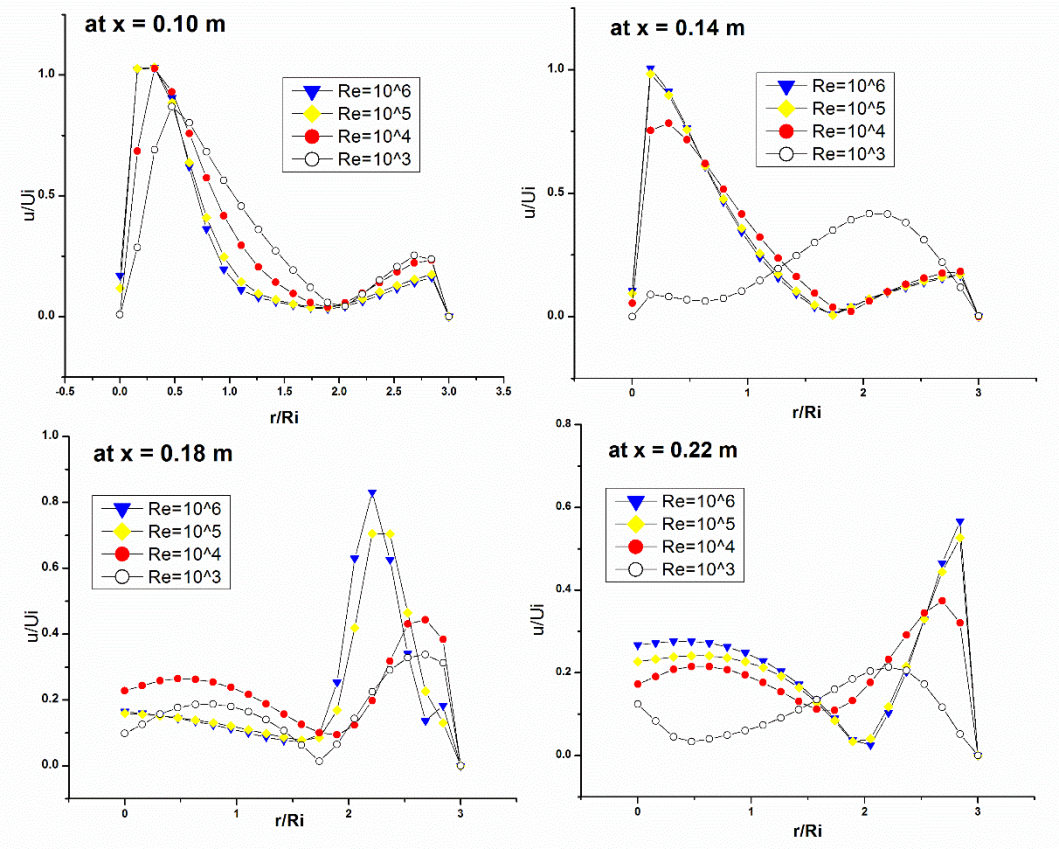

Figure 15. Variation of axial velocity profiles at different axial positions on x- axis for dump combustor with semi hemispherical restriction.

It has been noted that for axial location of 0.14 m, similar flow pattern is observed except for the Reynolds number of 10^3. The magnitude of velocity only increases slightly first and starts to decrease. It has been noted that, for Re of 10^3, the axial velocity increases and obtained its maximum value up to $^{r}/_{R_i}$ of 2 and becomes zero at the top of the wall.

From figure 15, for all Reynolds number, it has been noted that for axial location of 0.18 m, the magnitude of axial velocity initially increases a bit near centerline and then decreases and attains to zero velocity just before $^{r}/_{R_i}$ of 2. The peak value of axial velocity for Reynolds number 10^5 and 10^6 is obtained at $^{r}/_{R_i}$ of 2, and for Reynolds number 10^3 and 10^4, and it is achieved just near the top of the wall. It has also been observed that the spherical geometry of restriction affects the velocity distribution before and after the restriction. The plots show that velocity dips sharply as it approaches restriction and owing to the shape and curvature, it then gains kinetic energy during the downstream flow and increases again. This observation is caused due the same reasons stated in the above descriptions.

3.2.5 Dump combustor with diagonal restriction.

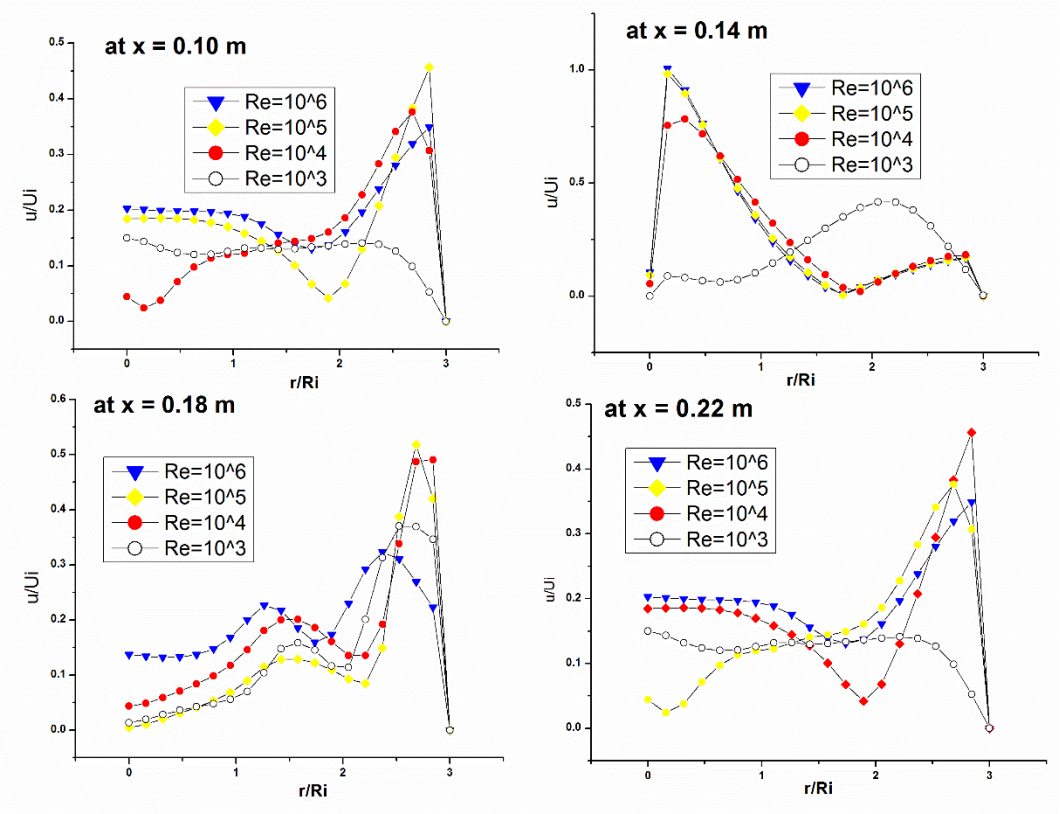

Figure 16. Variation of axial velocity profiles at different axial positions on x-axis for dump combustor with diagonal restriction.

Figure 16 depicts the variation of axial velocity for a dump combustor with diagonal restriction. All the curves show that axial velocity for Reynolds number 10^4 and 10^5 has its maximum value near the top wall of dump combustor (only for axial locations of 0.10 m, 0.18 m, and 0.22 m), than compared to Reynolds number 10^3 and 10^6. It is also noted that, for Reynolds number 10^5 and 10^6, axial location of 0.14 m, it gains its maximum value just after entrance of the combustor casing i.e. at $^{r}/_{R_i}$ of 0.3. For axial location of 0.10 m, considering Reynolds number 10^4, it is seen that the axial velocity first decreases a bit to zero and then increases up to top wall where its value is $^{u}/_{U_i}$ of 0.4. In case of Reynolds number 10^3, it is noted that the axial velocity starts at about $^{u}/_{U_i}$ of 0.15 and continues to smoothly decrease to zero at top wall. The value of axial velocity for Reynolds number 10^5 and 10^6 show similar trend except for Reynolds number 10^5 becomes zero just before $^{r}/_{R_i}$ of 2. For axial location of 0.14 m, it has been noted that peak value of maximum velocity for Reynolds number 10^3 is near the top wall ($^{u}/_{U_i}$ of 0.4), whereas for all other values of

Reynolds number it becomes zero just before $^{r}/_{R_i}$ of 2. From figure 16, it has also been noted that for axial locations of 0.10 m and 0.22 m, the axial velocity becomes zero just before $^{r}/_{R_i}$ of 2 for Reynolds number of 10^5 and 10^4 respectively. The reason behind these observations is due to the value of different inlet velocities and the diagonal restriction. From figure 16, it has been seen that for all considered Reynolds number, the magnitude of axial velocity initially increases a bit near centerline and then decreases and attains to zero velocity just before $^{r}/_{R_i}$ of 2 at axial location of 0.18 m. The peak value of axial velocity for Reynolds number 10^5 and 10^6 is obtained at $^{r}/_{R_i}$ of 2, and for Reynolds number 10^3 and 10^4, and it is achieved just near the top of the combustor wall.

3.3 Variation of axial velocities at centerline due to different restrictions:

Here, the limitation that impacts the velocity toward the exit is positioned around the centerline of the dump combustor, or the x-axis of the axisymmetric dump combustor. The flow velocity, its pattern, the size of the CRZ, and the quantity of recirculating bubbles created are all majorly determined by the central limitation and its shape. As it is evident from the Figure 17(a) that the maximum velocity attained in a simple annular dump combustor is for Reynolds number 10^3, which is essentially greater than inlet velocity. Key point to note in this case, is that the velocity starts to diminish more early for low Reynolds number. After a distance of 0.2m from the inlet manifold, the fluid's velocity starts to drop rapidly and increases a little just before the exit, in case of Re of 10^3.As for the greater Reynolds number, velocity inside combustor is constant for most part of combustor i.e. till 0.3 m length. It is worth mentioning that for Re=10^6, the final outlet velocity is much higher than that for Re of 10^3, which exits at a value of around 0.8 times the inlet velocity. In case of rectangular restriction, the height of restriction is 0.024 m (which is 1.2 times the inlet manifold) and horizontal length is 0.06 m. As Figure 17(b) depicts, the velocity just before the restriction wall becomes zero (at 0.14 m) and then gains momentum just when restriction ends, forming recirculating bubbles that leads to fluctuation in velocity till the outlet manifold. This drop and gain of velocity is an indicator of adequate mixing of fluid inside dump combustor, which cannot be seen in simple dump combustor. Here, the outlet velocity for Re=10^3 has a greater value.

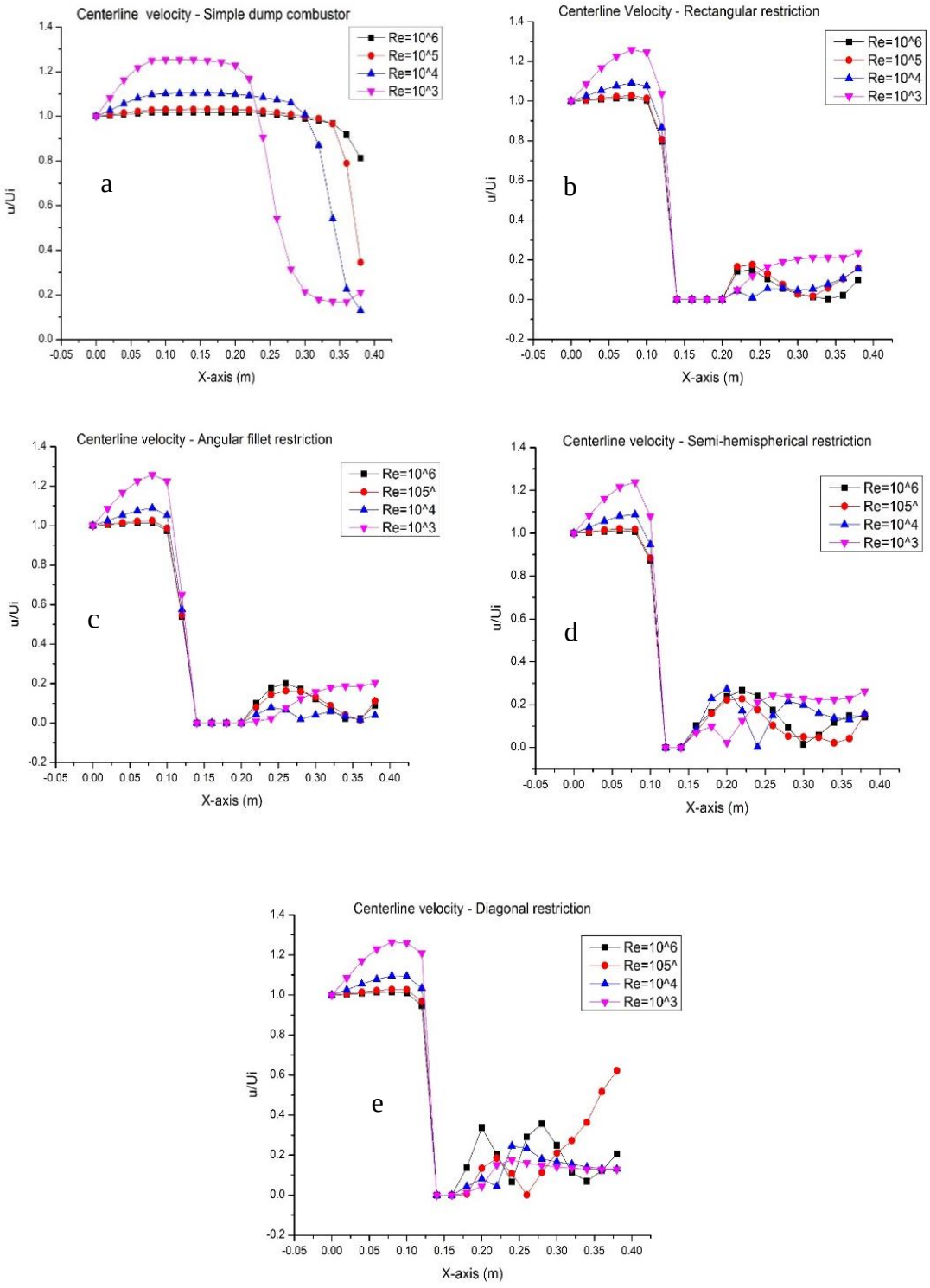

Figure 17. Variation of Centerline velocity for dump combustor without and with restriction.

Figure 17(c) depicts the centerline velocity variation for a rectangular curved combustor. A fillet of radius 0.024 m is added as a restriction to the previous geometry. The graph is similar in pattern to Figure 17(b). Here velocity after inside throat region is higher than inlet

velocity for Reynolds number 10^3. The final variation in velocities, after the fillet restriction, tend to show indistinguishable pattern from that of rectangular restriction's centerline velocity variation. Moreover, in both the type of rectangular modified dump combustors, the outlet velocity is highest when Reynolds number is taken as 10^3. The graph shows minimum central region mixing at low value of Reynolds number, whereas when Re is increased, rectangular restriction with added angular front wall reveals enhanced central mixing of fluid. There is potentially no fluid flow at corner above the throat at low value of Reynolds number, whereas as it is increased 1000 times, there is uniform distribution of CRZ all around the restriction, indicating proper mixing of combustion fluids and low probability of residuals from exhaust emission.

The centerline velocity variation depicted in figure 17(d), for spherical restriction clearly illustrates the fluctuation in velocities just before the outlet, which is caused due to more no. of recirculating bubbles and enlarged area of central recirculating zone, as confirmed from figure 8. However, as the restriction shape is altered and is more obstructive, it proves as am aid for better mixing of fluid-fuel mixture. Also the size of restriction gives more space for fluids to recirculate and allows convenient mixing and flow. Therefore, spherical restriction in a dump combustor would be most suitable, considering the size of restriction, for efficient mixing inside combustor casing.

The graphical representation for figure 17(e) of centerline velocity along the axis of dump combustor with diagonal restriction shows more fluctuation in velocities after passing the restriction. This follows only for high Reynolds number and interestingly, the outlet velocity is higher in this modified combustor for a Reynolds number of 10^5 as it exits as almost 0.6 times the inlet velocity. The variation of centerline velocity profiles shows similar pattern for all considered Reynolds number and for all dump combustors with various geometrical restrictions.

3.4 Variation of axial velocity profiles for different combustors at Re = 10^5:

A comparative study of simple dump combustor and modified dump combustor is depicted in figure 22. The figure illustrates the variation of axial velocity for simple dump combustor without restriction and modified dump combustors with certain geometrical modifications. From figure 22, it has been observed that, inlet velocity increases a bit up to r/R_i of 1, then it sharply starts descending till r/R_i of around 1.2. After that, the axial

velocity becomes zero and continues to be constant up to $^{r}/_{R_i}$ of 3.

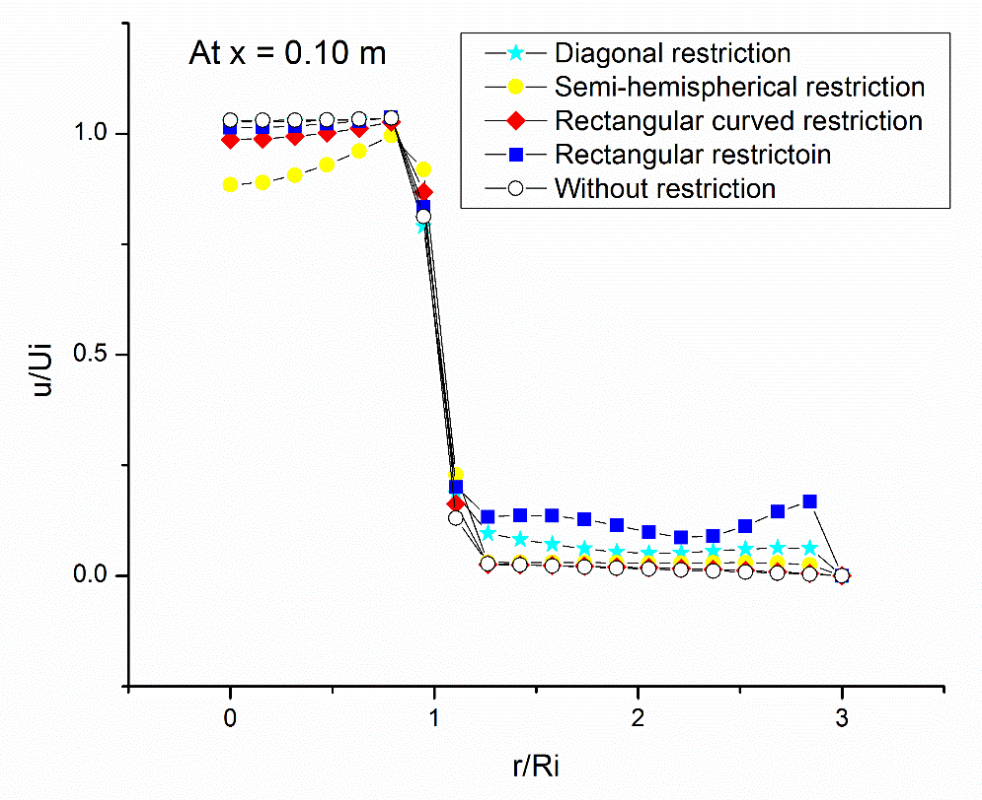

Figure 18. Variation of Axial velocity profile along the radial direction at x = 0.10 m.

However in case of semi-hemispherical and diagonal restriction, the velocity starts increasing at first up to $^{r}/_{R_i}$ of 1 and follows the curve as discussed above.It has also been noted that, the axial velocity before the outlet manifold, has certain positive magnitude in case of dump combustor with rectangular restriction. This observation may be accorded with the geometry of the restriction placed on the centerline.

CHAPTER 4

CONCLUSION

The analysis corroborates and concludes that there are more recirculating bubbles formed in a geometrically modified dump combustor than in a plain dump combustor. The geometry and position of restriction have a direct influence on the formation of recirculating zone. Additionally, as the Reynolds number is increased from 10^3 to 10^6, and as the restriction is made more flow-centric, there is a distinct change in no. of recirculating bubbles and a consistent mixing of fluid resulting in formation of an increased central recirculating zone.

Also there are more recirculating bubbles formed in dump combustors when provided with a restriction, showcasing the major CRZ near the restriction, top combustor wall and the central axis towards outlet, ensuring desirable mixing of fluid in combustor and low level of combustion residuals, which in turn helps increase engine efficiency in ship combustors. For effective and proper corner mixing, simple dump combustor and dump combustor with spherical and diagonal restriction show a dominant corner recirculating zone just above the throat, which vanishes on increasing Reynolds number to 10^5 and 10^6.

The maximum velocity in all modified dump combustors is found just next to the limitation front wall, where it dips sharply before rising again once the restriction has ended, signifying the establishment of a recirculating zone. The number of secondary RCZ between the restriction and outflow increases as the restriction geometry is altered and made more compact and flow-centric.

In this numerical investigation the flow characteristics of a fluid flowing through a simple annular dump combustor and modified dump combustor with certain central restrictions such as rectangular, curved, and spherical shapes are examined. It leads to the following conclusions.

1. More numbers of recirculating bubbles are formed in the modified combustors compared to simple dump combustors. It has also been mentioned that the large size of the bubble is formed at the central restriction zone.
2. The size of the vortex of the recirculating zone increases with increasing Reynolds number and the same is shifted towards the downstream side of the combustor.

Hence, it may be concluded that more number of recirculating bubbles and enlarged size of vortex in the central restriction zone robustly enhance the quality of mixing of fluids in the

modified dump combustor. Consequently, considerable reduction of temperature, NO_x formation, and combustion residual may be obtained. Therefore higher Reynolds number along with central restriction may be beneficial in terms of the design of the ship combustion chamber.

NOMENCLATURE

Alphanumeric symbols -

u_i Magnitude of inlet velocity, m/s

p_d Dynamic pressure, N/m

u Axial velocity (along x-axis)

v Transverse velocity (along y-axis)

k Turbulent kinetic energy

R_e Reynolds number

G Production constant

CRZ Central recirculating zone

AR Aspect Ratio

C_{mu}, $C_{1\varepsilon}$, and $C_{2\varepsilon}$ Turbulent constants

D_i Diameter of inlet manifold

p_{d-in} Dynamic pressure at inlet

Greek characters-

ρ Density, kg/m^3

μ Dynamic viscosity, kg/m-s

μ_t Turbulent viscosity, kg/m-s

τ_x Turbulent stress tensor along x-axis

τ_y Turbulent stress tensor along y-axis

ε Turbulent dissipation rate or rate of dissipation of turbulent kinetic energy due to viscous effects.

PUBLICATIONS FROM THIS THESIS

- Vaibhav Soni and Sujoy Saha, 2022**, "Numerical design on annular dump combustor of a Ship"**, *International conference on Research in Advanced Fluid Mechanics (ICRAFM 2022)*, Manipal University, (Accepted)
- V. Soni and S. Saha, 2022**, "Effect of Central Restriction on Dump Combustor Design"**, *International Journal of Thermofluid Science and Technology*, (Communicated)

REFERENCES

Patankar, S. V., 1980, "**Numerical Heat Transfer and Fluid Flow**", Hemisphere Publication.

Tsui, Y.Y.., and Shu, S. J., 1998, "**Effect of Bouyancy and Orientation on the Flow in a Duct Preceded with a double-step expansion**", *Int. J. Heat Transfer*, 41(17):2687 – 2695.

Hammad, K. J., Otugen, M. V., Vradis, G. C. and Arik, E. B., 1999, "**Laminar Flow of a Nonlinear Viscoplastic Fluid Through an Axisymmetric Sudden Expansion**", *ASME, Journal of Fluids Engineering*, 121:488-495.

Khezzar, L., De Zilwa, S. R. N., Whitelaw, J.H., 1999, "**Combustion of premixed fuel and air downstream of a plane sudden-expansion**", *Experiments in Fluids*, 27:296-309.

Yokoyama, Y., Kulacki, F. A. and Mahajan, R. L., 1999, "**Mixed Convection in a Horizontal Porous Duct with a Sudden Expansion and Local Heating from Below**", *ASME, Journal of Heat Transfer*, 121:653-661.

Tavoularis, S., Singh, R. K., 1999, "**Vortex Detachment and Reverse Flow in Pulsatile Laminar Flow through Axisymmetric Sudden Expansions**", *ASME, Journal of Fluids Engineering*, 121:574-579.

Schreck, E., and Schafer, M., 2000, "**Numerical study of bifurcation in three-dimensional sudden channel expansions**", *Computers & Fluids*, 29:583-593.

Guo, B., Langrish, T. A. G. and Fletcher, D. F., 2001, "**Numerical Simulation of Unsteady Turbulent Flow in Axisymmetric Sudden Expansions**", *ASME, Journal of Fluids Engineering*, 123:574-587.

Chakrabarti, S., Ray, S., and Sarkar, A., 2002, "**Numerical Simulation of the Performance of a Vortex Controlled Diffuser in Low Reynolds Number Regime**", *International Journal of Numerical Methods for Heat & Fluid Flow*, 12(3):224-240.

Paschereit, C. O. and Gutmark, E. J., 2002, "**Enhanced Performance of a Gas-Turbine Combustor Using Miniature Vortex Generators**"*Proceedings of the Combustion Institute*, 29:123–129.

Galvin, S. and Fitzpatrick, J.A., 2002, "**Thermo-Acoustic Interactions in a Premixed Dump Combustor**", *ASME Proceedings of International Mechanical Engineering Congress and Exposition*, IMECE2002-33358:1-8.

Pinho, F. T., Oliveira, P. J., and Miranda, J. P., 2003, "**Pressure losses in the laminar flow of shear-thinning power-law fluids across a sudden axisymmetric expansion**", *Int. J. Heat and Fluid Flow*, 24:747-761.

Smith, B.L., 2004, "**Pressure recovery in a rediused sudden expansion",** *Experiments in Fluids*, 36:901-907.

Behrens, A. A., Anderson, M. J., Strykowski, P. J. and Forliti, D. J., 2005, "**Enhancing Combustion in a Dump Combustor Using Countercurrent Shear. Part 2: Heat Release Rate Measurements and Geometry Effects**", *ASME Proceedings of International Mechanical Engineering Congress and Exposition*, IMECE2005-81274:1-8.

Forliti, D. J., Behrens, A. A., Strykowski, P. J. and Tang, B. A., 2005, "**Enhancing Combustion In A Dump Combustor Using Countercurrent Shear. Part 1: Nonreacting Flow Control And Preliminary Combustion Results**", *ASME Proceedings of International Mechanical Engineering Congress and Exposition*, IMECE 2005-81267:1-8.

Palm, R., Grundmann, S., Weismüller M., šaric´, S., Jakirlic´, S. and Tropea, C., 2006, "**Experimental characterization and modelling of inflow conditions for a gas turbine swirl combustor**", *International Journal of Heat and Fluid Flow*, 27:924–936.

Abu-Nada, E., Al-Sarkhi, A., Akash, B. and Al-Hinti, I., 2007, "**Heat Transfer and Fluid Flow Characteristics of Separated Flows Encountered in a Backward-Facing Step under the Effect of Suction and Blowing**", *ASME, Journal of Heat Transfer*, 129:1517-1528.

Duwig, C. and Fureby, C., 2007, "**Large eddy simulation of unsteady lean stratified premixed combustion**", *Combustion and Flame*, 151:85–103.

Kodama, K., Toda, K., and Yamamoto, M., 2007, "**Investigation on RANS Computation for an Unsteady Turbulent Flow (In the Case of a Backward Facing Step Flow with Periodic Perturbation)**", *JSME, J. Fluid Science and Technology*, 2(3):623 – 632.

Strakey, P. A. and Yip, M. J., 2007, "**Experimental and Numerical Investigation of a**

Swirl Stabilized Premixed Combustor Under Cold-Flow Conditions", *ASME, J. Fluids Engg.*, 129:942 - 953.

Uruba, V., Jona´sˇ, P. and Mazur, O., 2007, "**Control of a channel-flow behind a backward-facing step by suction/blowing**", *International Journal of Heat and Fluid Flow*, 28:665–672.

Vanierschot, M. and Van den Bulck, E., 2007, "**Hysteresis in flow patterns in annular swirling jets**", *Experimental Thermal and Fluid Science*, 31:513–524.

Chakrabarti S., Ray S. and Sarkar A., 2008, "**Numerical analysis for sudden expansion with fence in low Reynolds number regime**"; *J. Energy, Heat and Mass Transfer*, 30:131-148.

Layek, G. C., Midya, C., Mukhopadhyay, S., 2008, "**Effects of Suction and Blowing on Flow Separation in a Symmetric Sudden Expanded Channel**", *Nonlinear Analysis: Modelling and Control*, 13(4):451–465.

Nguyen, P. D., Bruel, P., and Reichstadt, S., 2008, "**An Experimental Database for Benchmarking Simulations of Turbulent Premixed Reacting Flows: Lean Extinction Limits and Velocity Field Measurements in a Dump Combustor**", *Flow Turbulence Combust*, DOI 10.1007/s10494-008-9160-4.

Tsai, G. L., Lin, Y. C., Wang, H.W., Lin, Y. F., Su, Y. C. and Yang, J. T., 2009, "**Cooling transients in a sudden-expansion channel with varied rates of wall transpiration**", *International Journal of Heat and Mass Transfer*, 52:5990–5999.

Ayache, S., Dawson, J. R., Triantafyllidis, A., Balachandran, R. and Mastorakos, E., 2010, "**Experiments and Large-Eddy Simulations of acoustically forced bluff-body flows**", *International Journal of Heat and Fluid Flow*, 31:754–766.

Zohir, A.E., Abdel Aziz, A.A. and Habib, M.A., 2011, "**Heat transfer characteristics in a sudden expansion pipe equipped with swirl generators**", *International Journal of Heat and Fluid Flow*, 32:352–361.

Banerjee, N., Mondal, D. K. and Chakrabarti, S., 2011, "**A Numerical Experimentation on the Performance of a Sudden Expansion with Two Fences in Terms of Static Pressure Rise When Viewed as a Diffuser**", *Proceedings of the International Conferences on Design and Advances in Mechanical Engineering*, 706-712.

Fattah, A., 2012, "**Control of the Separation Flow in a Sudden Enlargement**", *Journal of Applied Fluid Mechanics*, 5(1):57-66.

Tsai, C. H., Yeh, C. P., Lin, C. H., Yang, R. J. and Fu, L. M., 2012, "**Formation of**

recirculation zones in a sudden expansion microchannel with a rectangular block structure over a wide Reynolds number range", *Microfluid Nanofluid*, 12:213-220.

Kim, K. T.and Santavicca, D. A., 2013, "**Interference mechanisms of acoustic/convective disturbances in a swirl-stabilized lean-premixed combustor**", *Combustion and Flame*, 160:1441-1457.

Baig, M. A. A. and Khan, S. A., 2012, "**Studies on Suddenly Expanded Flow at Different Levels of Over Expansion for Area Ratio 3.24**" *International Journal of Scientific & Engineering Research*, 3(6):1-5.

Tuncer, O., Kaynarog˘lu, B., Karakaya, M. C., Kahraman, S., Yıldırım, O. C. and Baytas C., 2014, "**Preliminary investigation of a swirl stabilized premixed combustor**", *Fuel*, 115: 870–874.

Saha S, Chakrabarti S. 2016**,"MHD Modelling and Numerical Simulation on ferromagnetic Fluid Flow in a Channel",** International Journal of Fluid Mechanics Research. 43(1): 79-92.

Saha S, and Chakrabarti S. 2020, **"Numerical Simulation on the Magnetic Fluid Flow through a Channel"**, Indian Journal of Engineering. 17(47):117-126.

Launder B. E., Spalding D. B., 1997, The Numerical Computation of turbulent flows Computer method in Appl. Mech. and Engg. 03 269-289